CAPITAL UNIVERSITY OF SCIENCE AND TECHNOLOGY, ISLAMABAD

MHD boundary layer flow of Williamson nanofluid with the effect of Cattaneo-Christov heat flux

by

Naveeda Aziz

A thesis submitted in partial fulfillment for the degree of Master of Science

in the

Faculty of Computing

Department of Mathematics

2018

Copyright © 2018 by Naveeda Aziz

All rights reserved. No part of this thesis may be reproduced, distributed, or transmitted in any form or by any means, including photocopying, recording, or other electronic or mechanical methods, by any information storage and retrieval system without the prior written permission of the author.

I dedicate this Sincere effort to my dear ***Parents****, my elegant* ***Teachers****, and my Superisor* ***Dr. Shafqat Hussain*** *who are always source of Inspiration for me and their contributions are uncounted.*

CAPITAL UNIVERSITY OF SCIENCE & TECHNOLOGY
ISLAMABAD

CERTIFICATE OF APPROVAL

MHD boundary layer flow of Williamson nanofluid with the effect of Cattaneo-Christov heat flux

by

Naveeda Aziz
MMT153001

THESIS EXAMINING COMMITTEE

S. No.	Examiner	Name	Organization
(a)	External Examiner	Dr. Kamran Usman	AIR, Islamabad
(b)	Internal Examiner	Dr. Muhammad Sagheer	CUST, Islamabad
(c)	Supervisor	Dr. Shafqat Hussain	CUST, Islamabad

Dr. Shafqat Hussain
Thesis Supervisor
January, 2018

Dr. Muhammad Sagheer
Head
Dept. of Mathematics
January, 2018

Dr. Muhammad Abdul Qadir
Dean
Faculty of Computing
January, 2018

Author's Declaration

I, **Naveeda Aziz** here by state that my MS thesis titled "**MHD boundary layer flow of Williamson nanofluid with the effect of Cattaneo-Christov heat flux**" is my own work and has not been submitted previously by me for taking any degree from Capital University of Science and Technology, Islamabad or anywhere else in the country/abroad.

At any time if my statement is found to be incorrect even after my graduation, the University has the right to withdraw my MS Degree.

(Naveeda Aziz)

Registration No: MMT153001

Plagiarism Undertaking

I solemnly declare that research work presented in this thesis titled "*MHD boundary layer flow of Williamson nanofluid with the effect of Cattaneo-Christov heat flux*" is solely my research work with no significant contribution from any other person. Small contribution/help wherever taken has been dully acknowledged and that complete thesis has been written by me.

I understand the zero tolerance policy of the HEC and Capital University of Science and Technology towards plagiarism. Therefore, I as an author of the above titled thesis declare that no portion of my thesis has been plagiarized and any material used as reference is properly referred/cited.

I undertake that if I am found guilty of any formal plagiarism in the above titled thesis even after award of MS Degree, the University reserves the right to withdraw/revoke my MS degree and that HEC and the University have the right to publish my name on the HEC/University website on which names of students are placed who submitted plagiarized work.

(Naveeda Aziz)

Registration No: MMT153001

Acknowledgements

In the name of **ALLAH**, the Most Gracious and the Most Merciful, all praise is for **ALLAH**; we praise Him, seek His help, and ask for His forgiveness. I am thankful to **ALLAH**, who gave me the courage, the guidance, and helped me throughout incompleting the research. Also, I cannot forget the ideal man of the world and most respectable personality for whom **ALLAH** created the whole universe, Prophet Muhammad (Peace Be Upon Him).

Foremost, I would like to express my heart-felt gratitude to most cooperative and good communicator my supervisor **Dr. Shafqat Hussain**, Associate Professor, Capital University of Sciences and Technology, Islamabad who suggested the problem. The doors towards supervisor were always opened whenever I ran into a trouble spot. His guidance helped me in all the time of research and writing of this thesis. He has always helped me out and tolerated my untimely disturbances. He consistently allowed this thesis to be my own work, but steered me in the right direction whenever he thought I need it.

This segment would be incomplete without referring to very generous and noble person **Dr. Muhammad Sagheer**, Professor, Capital University of Science and Technology, for his continuous encouragement, motivation and moral assistance.

The acknowledgement will surely remain incomplete if I don't express my deep indebtedness and cordial thanks to **Maleeha Atlas**, the Ph.D scholar of department of mathematics for her valuable suggestions, guidance and unendindg cooperation during my thesis.

I would like to acknowledge CUST for providing me such a favourable environment to conduct this research.

I must express my very profound gratitude to my dear parents and whole members of my family including my younger brothers **Sardar Imran, Sardar Irfan** and **Sardar Ayyan**, and my dear sisters and my cousins, friends and room mates for providing me with unfailing support and continuous encouragement throughout my years of study and through the process of researching and writing this thesis. This accomplishment would not have been possible without them.

Abstract

The main objective of this dissertation is to focus on a numerical study of chemical reaction and radiation effects on the steady state boundary layer flow of MHD Williamson nanofluid in a porous medium past the horizontaly stretching sheet with the existence of nanoparticles. Moreover, the impact of Cattaneo-Christov heat flux model is also discussed. A mathematical model which resembles the physical flow problem has been developed. Similarity transformations are used to convert partial differential equations (PDEs) into a system of nonlinear ordinary differential equations (ODEs). The resulting system of ordinary differential equations (ODEs) is solved numerically by using shooting method and obtained numerical results are compared with Matlab bvp4c built in function, which shows an excellent agreement. Effects of various physical parameters on the dimensionless velocity, temprature, and concntration profiles are shown in the form of graphs. Numerical values of skin friction coefficient, Nusselt number (heat transfer rate), and Sherwood number (mass transfer rate) are also computed. The effects of different physical parameters on the flow and heat transfer characteristics are discussed in detail.

Contents

List of Figures

List of Tables

Abbreviations

MHD	Magnetohydrodynamics
PDEs	partial differential equations
ODEs	ordinary differential equations
RK	Runge-Kutta
IVPs	initial value problems
BVPs	boundary value problems

Symbols

(u, v)	velocity components
(x, y)	cartesian coordinates
ρ	nanofluid density
ν	kinematic viscosity
ψ	stream function
θ	nondimensional temperature
ϕ	nondimensional concentration
D_B	coefficient of Brownian diffusion
D_T	coefficient of thermophoresis diffusion
k'	porous medium permeability
B_0	induced magnetic field
T_w	nanofluid temperature near wall
T_∞	free stream temperature of nanofluid
λ	non-Newtonian Williamson parameter
k_p	permeability parameter
Pr	Prandtl number
Nu	Nusselt number
R	radiation parameter
Nb	Brownian motion parameter
Nt	thermophoresis parameter
Le	Lewis number
γ	chemical reaction parameter
M	dimensionless melting parameter

k^*	mean absorption coefficient
ξ	dimensionless similarity variable
C_f	skin friction coefficient
Sh	Sherwood number
q_w	surface heat flux
q_m	surface mass flux
Re	Reynolds number
κ	thermal conductivity
$(\rho c)_f$	heat capacity of the fluid
$(\rho c)_p$	heat capacity of the nanoparticle

Chapter 1

Introduction

A substance in the gas or liquid phase is referred to as the fluid. Flow of fluid has all kinds of aspects, steady and unsteady, compressible and incompressible, viscous and inviscid, rotational and irrotational, uniform and non-uniform etc, Meir [1]. The study of fluid flow on a stretching sheet is one of the important problems in the current era as it occurs in different processes of engineering for example, extrusion, wire drawing, food manufacturing, metal spinning, manufacturing of rubber sheets and cooling of huge metallic plates such as an electrolyte, etc. Sakiadis [2] was the first who introduced the problem of boundary layer approximations over stretching surface. The flow caused by stretching sheet was investigated by Crane [3]. Recently, many researchers such as Shehzad *et al.* [4], Zheng *et al.* [5], and Gireesha *et al.* [6] are interested to investigate the fluid flow phenomenon passed through stretching surfaces because of significant applications as mentioned above.

Heat transfer, is the thermal energy movement from one system to another system at various temperatures. There are three mechanisms of transfer of heat: convection (through fluid movement), radiation (through electromagnetic waves), or conduction (through direct contact). It is a well known fact that the phenomenon of heat transfer occurs between two bodies (or within the same body) due to the difference of temperature. The research of flow and heat transfer generated by means of stretching medium has plenty of significance in numerous industrialized

developments, e.g, in the process of rubber and plastic sheets manufacturing, upgrading the solid materials like crystal, turning fibers etc. The most widely used coolant liquid among them is water. In the above cases, the heat transfer and flow investigation are of significant importance because the final product quality be determined to bulk level on the basis of coefficient of skin friction and heat transfer surface rate. In various industrial processes of engineering, the characteristics of heat transfer have huge demands in microelectronics, transportation and fuel cells etc. Numerous investigators have analyzed different traits of stretching flow problem. Elbashbeshy [7] studied about transfer heat and flow of viscous fluid by assuming the stretched sheet. After that Sanjayanand and Khan [8] extended their work about mass and heat transfer of viscoelastic fluid by assuming the elastic deformation and viscous dissipation. The numerical results for mass and transfer of heat of viscous fluid about stretching sheet were developed by Magyari and Keller [9].

Nanoparticles are particles between 1 and 100 nanometer in size. Nanofluids are obtained through dispersion of nanoparticles with base fluid usually (water). The purpose of nanofluids is to approach the maximum thermal properties with smallest possible concentration. The development of nanofluids helped to achieve superior thermal conductivity and enhanced heat transfer characteristics. Nanofluids are homogenous mixture of nanoparticles and the base fluid. Some common nanoparticles include carbons in different forms like diamond and grphite carbon nanotubes, Aluminium Oxide (Al_2O_3), Copper Oxide (CuO), Aluminium Nitride (AlN), Silcon Nitride (SiN), etc. All nonmetallic and metallic particles change the transfer properties and heat conduction characteristics of the base fluids for example, liquids of organic, refrigerants, ethylene, etc. In fact the enhanced thermal conductivity is based on the nanoparticles while the effectiveness of heat transfer enhancement also depends upon the dispersed particles, material type, etc. The use of additives is another way to enhance the heat transfer capacity of base fluid. Recent research proved that such techniques can improve the heat transport characteristics and thermal conductivity of the base fluid and consequently the efficiency of energy. The research on the enhancement of thermal properties of

conventional base fluid was introduced by Choi [10] in 1995. Choi *et al.* [11] indicated the major fact that thermal conductivity of the conventional heat transfer liquids increased up to approximately two times by adding the small amount of nanoparticles in the fluid, that is, less than 1 by volume. Khanafer *et al.* [12] investigated nanofluids heat transport inside an enclosure for the solid particles dissipation.

The study of magnetic properties of electrically conducting fluids is known as Magnetohydrodynamics (MHD). MHD fluid flow was first introduced by Swedish Physicist, Alfven [13]. In recent years, mass and heat transfer on unsteady MHD natural convenction rotating flow of fluid about a porous plate with heat transfer and radiation was studied by Mbeledogu and Ogulu [14]. Kesavaiah *et al* [15] investigated the unsteady MHD convective flow over a vertical porous plate. The effect of convection in MHD flow of Jeffrey fluid of heat transfer about a stretching sheet is reported by Hayat *et al.* [16]. Mustafa *et al.* [17] inspected the MHD Maxwell fluid flow with convective heat transfer. MHD viscous incompressible flow has many applications in engineering for example, cooling of reactors, a power generator, MHD accelerators and design of heat exchangers, as provoked by Hari *et al* [18].

Non-Newtonian fluids are those for which the shear stress is not linearly proportional to the deformation rate. In other words, fluids that do not satisfy Newton's law of viscosity are known as non-Newtonian fluids. Blood, paints, ketchup, shampoo, mud etc, behave like non-Newtonian fluids. Williamson fluid is one of non-Newtonian fluids. The study of Williamson fluids for the boundary layer flow is of great interest because of its vast range of applications in different branches of science, technology and engineering, especially material processing, in nuclear and chemical industries, bio-engineering and geophysics. Considering, these applications an extensive range of mathematical models has been developed to simulate the flow behavior of these non-Newtonian fluids. Williamson [19] discussed the flow of pseudoplastic materials and presented a model equation to discuss the pseudoplastic fluids flow and verified the results experimentally. Nadeem *et al.* [20] presented the Williamson fluid flow past a stretching surface and found

that by increasing values of Williamson fluid parameter, the dimensionless velocity decreases. Heat transfer characteristics on non-Newtonian nanofluid flow over a stretching sheet was presented by Nadeem and Hussain [21]. Hayat and Hina [22] studied the impact of mass and heat transfer with flexible walls on Williamson fluid flow. In current era, Hayat *et al.* [23] presented a study to analyze the impact of Ohmic heating in peristaltic flow of non-Newtonian fluid. Initially, Sarpakaya [24] investigated the non-Newtonian fluid flows in the presence of magnetic field. He introduced two non-Newtonian models known as power-law model and Bingham plastic model for the influence of magnetic field. Recently, flows of boundary layer of Newtonian and non-Newtonian fluids have drawn considerable attention because of their significant applications in processing of metallurgical, phenomena of chemical engineering transport, molten polymers extrusion, plastic sheets and wrapping foils fabrication etc. Species, momentum and heat transport play a major role in such processes [25]. Qasim introduced the impact of mass and heat transfer on non-Newtonian Jeffrey viscoelastic fluid flow in the existence of heat source/sink [26]. A mathematical model to investigate the impact of melting heat transfer non-Newtonian fluid flow in porous medium with Lorentz force was given by Krishnamurthy *et al.* [27].

The law of Fourier of heat conduction [28] has been the typical approach for thermal conduction and simulation of heat transfer. The major disadvantage of this model however, is that it converts the heat conservation formulation to parabolic energy equation which indicates that the medium under consideration experiences an initial disturbance. Cattaneo [29] introduced a relaxation time term in heat conduction law of Fourier's to overcome this difficulty. Afterwards, Christov [30] changed the law of Cattaneo by time derivative in Maxwell-Cattaneo's model with Oldroyd's upper-convected derivative to conserve material-invariant formulation. Starzewski [31] used the model of Cattaneo-Christov to analyze thermal convection in flow of incompressible fluid. Tibullo and Zampoli [32] analyzed the uniqueness of Cattaneo-Christov heat flux model for flow of incompressible fluid. Khan *et al.* [33] numerically investigated the heat flux model of Cattaneo-Christov in viscoelastic flow due to stretched sheet.

1.1 Thesis contribution

In this dissertation, a review study of Krishnamurthy *et al.* [27] has been presented and then the flow analysis has been extended with variable thermophysical properties. The governing system of nonlinear PDEs is converted into a system of nonlinear coupled ODEs by utilizing appropriate similarity transformation. Numerical results are obtained for the set of nonlinear coupled ODEs by using shooting technique and numerical results are compared through the MATLAB built-in function bvp4c. The numerical results are analyzed for different parameters through graphs and tables.

1.2 Outline of the dissertation

This thesis further consists of four chapters.

Chapter 2 presents some basic definitions, terminologies and the governing laws. We also explain the solution methodology used in this thesis.

Chapter 3 contains a comprehensive review of Krishnamurthy *et al.* [27]. This chapter is related to the problem formulation. To obtain the numerical solutions, the PDEs (nonlinear) have been converted to a system of ODEs (nonlinear) using similarity transformation. Later on the system of nonlinear coupled ODEs is solved by using shooting technique. The obtained numerical solutions are also compared with MATLAB built-in function bvp4c.

Chapter 4 extends the work of Krishnamurthy *et al.* [27] by considering the Cattaneo-Christov heat flux model. By utilizing similarity transformation we reduce the set of nonlinear PDEs into a set of nonlinear ODEs and then solve numerically. Graphs and tables describe the behavior of physical parameters.

Chapter 5 contains thesis summary and gives the outcome achieved from the entire research and suggests future recommendations.

All the references used in this thesis are presented in **Bibliography**.

Chapter 2

Basic definitions and governing equations

In this unit, some basic definitions, terminologies and governing laws will be presented, which will be helpful in continuing the work for the next units [1].

2.1 Some basic definitions

Definition 2.1.1. (Fluid)

Fluid is a class of matter which deforms continuously under the influence of shear stress.

Definition 2.1.2. (Fluid mechanics)

Fluid mechanics deals with the study of laws of force and properties of fluid and the effect of forces on it. It can further be divided into two categories presented next.

Definition 2.1.3. (Fluid statics)

In fluid statics, we study the behavior of fluids at the state of rest. It is also referred to as hydrostatics.

Definition 2.1.4. (Fluid dynamics)

The branch that covers the properties of fluid in the state of progression from one place to another is called fluid dynamics.

Definition 2.1.5. (Viscosity)

The fluid property that measures the resistance to flow. It is denoted by μ.

Definition 2.1.6. (Dynamic Viscosity)

The fluid property that measures the internal resistance of fluid is called dynamic viscosity. This resistance arises from the attractive forces between the molecules of the fluid, and it is denoted by μ. Mathematically, it is written as:

$$\mu = \frac{\text{Shear stress}}{\text{Rate of shear strain}}.$$

In the above expression μ is called the coefficient of viscosity, also known as absolute viscosity having dimension $[ML^{-1}T^{-1}]$. Unit of viscosity in SI system is kg/ms or Pascal-second [Pa.s].

Definition 2.1.7. (Kinematic viscosity)

The kinematic viscosity depicts the ratio between dynamic viscosity μ and the fluid density ρ. It is represented by ν and mathematically, it can be expressed as:

$$\nu = \frac{\mu}{\rho}.$$

The dimension of kinematic viscosity is $[L^2T^{-1}]$ and its unit in SI system is m^2/s.

2.2 Classification of fluids

Definition 2.2.1. (Ideal fluid)

The fluid which has no viscosity ($\mu = 0$) is known as an Ideal fluid. It is also called inviscid fluid. There is no existence of shear force because the viscosity is vanishing in an ideal fluid.

Definition 2.2.2. (Real fluid)

The fluid containing some viscosity effect is said to be a real or viscous fluid having ($\mu > 0$).

Definition 2.2.3. (Nanofluid)

The nanofluid is defined as the homogenous mixture of the base fluid and nanoparticles. The purpose of the nanofluids is to achieve high thermal properties at the smallest concentration.

Definition 2.2.4. (Newtonian fluids)

A fluid in which the viscous stresses arise from its flow and linearly proportional to the strain, i.e., the rate of change of its deformation, as shear stress and the rate of deformation are directly proportional to each other, is called a Newtonian fluid. On the other hand, the fluids which obey the Newtons law of viscosity are called Newtonian fluids. Mathematically, defined as

$$\tau_{yx} = \mu \frac{du}{dy},$$

where τ_{yx} is the shear stress, u denotes the x-component of velocity, and μ denotes dynamic viscosity. The common examples of Newtonian fluids are air, water, alchohols, oxygen gas, and silicone etc.

Definition 2.2.5. (Non-Newtonian fluid)

Those fluids for which the shear stress is not linearly proportional to the rate of deformation. In other words, the fluid which does not satisfy the Newtons law of viscosity is also said to be non-Newtonian fluid, mathematically written as:

$$\tau_{xy} \propto \left(\frac{du}{dy}\right)^n, \ n \neq 1$$

$$\tau_{xy} = \mu \left(\frac{du}{dy}\right)^n,$$

where μ denotes the viscosity, n is the index of flow performance. Note that for $n = 1$, the above equation reduces to the Newtons law of viscosity. Examples of non-Newtonian fluids are shampoo, grease, paint, blood and melt polymer etc.

2.3 Types of flow

Definition 2.3.1. (Flow)

The random motion of a fluid is known as flow. Different types of flow are given as follows:

Definition 2.3.2. (Laminar flow)

Regular flow of a fluid is known as laminar flow. Rising of smoke is an example of laminar flow.

Definition 2.3.3. (Turbulent flow)

When fluid undergoes irregular fluctuations or flowing faster, this type of fluid (liquid or gas) is called turbulent flow. Turbulent flow which moves randomly in any direction and has no definite path and can't be handled easily. It undergoes changes both in magnitude and direction.

Definition 2.3.4. (Uniform flow)

The flow in which the velocity and hydrodynamic parameters do not change from point to point at any given instant, having the same direction as well as magnitude during the fluid motion, is called the uniform flow. Mathematically, it can be expressed as

$$\frac{d\mathbf{V}}{ds} = 0,$$

where $\mathbf{V}$ is the velocity and s is the displacement.

Definition 2.3.5. (Non-uniform flow)

In non-uniform flow, the velocity and hydrodynamic parameters change from one point to another point and the velocity is not same at every point of the fluid at an instant. Mathematically, it is expressed as

$$\frac{d\mathbf{V}}{ds} \neq 0,$$

where $\mathbf{V}$ is the velocity and s is the displacement in any direction.

Definition 2.3.6. (External flow)

The flow which is not bounded by the solid surface is called external flow. For example, the flow of water in the river.

Definition 2.3.7. (Internal flow)

The flow is bounded and confined by the solid surface and convenient geometry for cooling and heating fluids used in the energy is called as internal flow. e.g, flow in a pipe.

Definition 2.3.8. (Steady flow)

The flow having no change with respect to time is said to be steady flow. Mathematically, it can be written as

$$\frac{\partial B}{\partial t} = 0,$$

where B is any fluid property.

Definition 2.3.9. (Unsteady flow)

The flow in which fluid properties change with respect to time is said to be unsteady flow. Mathematically, it can be written as:

$$\frac{\partial B}{\partial t} \neq 0,$$

here B is any fluid property.

Definition 2.3.10. (Compressible flow)

The density of certain fluids changes with the variation in temperature or pressure, such a fluid is called compressible fluid. In other words, we can say that density with respect to certain variables does not remain constant, and mathematically, written as:

$$\rho(x, y, z, t) \neq \text{constant}.$$

Definition 2.3.11. (Incompressible flow)

The density of certain fluid does not change with the variation in temperature or pressure, such a fluid is known as incompressible fluid. In other words, we can say that density of such fluids remain constant, mathematically written as:

$$\rho(x, y, z, t) = \text{constant}.$$

2.4 Heat transfer

The energy transfer is called heat transfer. There are three types of heat transfer:

Definition 2.4.1. (Conduction)

Due to collision of molecules in contact form, heat is transferred from one objects to another objects is called conduction. Such types of heat transfer occurs in the solid.

Definition 2.4.2. (Convection)

Convection which is produced by heat transport process by an external source is known as convection. In other words, heat transfer technique in which fluid motion is developed by an independent source like a fan and pump etc. is known as convection.

Definition 2.4.4. (Mixed convection)

It occurs by the combined influence of forced and natural convection to transfer heat. In other words, when both natural and forced convection processes simultaneously contribute to cause the heat transfer, mixed convection occurs.

Definition 2.4.5. (Natural convection)

It is the process, in which heat transfer is caused by the temperature differences. It effects the density of the fluids and the fluid motion is not developed by an external source. It occurs only in the presence of gravitational force and also known as free convection.

Definition 2.4.6. (Radiation)

The process in which heat is transmitted directly through the electromagnetic radiation, is known as radiation and it happens in those situations when bodies having different temperature are placed such that they have sight line among their surfaces.

Definition 2.4.7. (Thermal conductivity)

It is the material property related to its capability to transmit heat. Mathematically,

$$\kappa = \frac{q\nabla l}{S\nabla T},$$

where q represents heat passing through a surface area S and causing a temperature difference ∇T over a distance of ∇l. Here l, S and ∇T all are assumed to have unit measurement. In SI the unit of thermal conductivity is $\frac{W}{m.\kappa}$ and its dimension is $[MLT^{-3}\theta^{-1}]$.

Definition 2.4.8. (Thermal diffusivity)

Thermal diffusivity is a material property for unsteady heat conduction. Mathematically, it can be written as:

$$\alpha = \frac{\kappa}{\rho C_p},$$

where κ, ρ and C_p denote the thermal conductivity of material, the density and the specific heat capacity respectively. The unit and dimension of thermal diffusivity in SI system are m^2s^{-1} and $[L^2T^{-1}]$ respectively.

2.5 Dimensionless numbers

Definition 2.5.1. (Prandtl number)

This number has no dimension. It is the ratio between the momentum diffusivity (ν) and thermal diffusivity (α). It is denoted by Pr. Mathematically, it can be written as:

$$Pr = \frac{\nu}{\alpha} \quad \Longrightarrow \quad \frac{\mu/\rho}{k/\rho C_p} \quad \Longrightarrow \quad \frac{\mu C_p}{k},$$

where μ denotes the dynamic viscosity, C_p represents the specific heat and κ stands for the thermal conductivity.

Definition 2.5.2. (Lewis number)

The Lewis number can be defined as the ratio of the thermal diffusivity to the molecular diffusivity. It helps us to find the relationship between mass and heat transfer coefficient. It is denoted by Le. Mathematically,

$$Le = \frac{\lambda}{\rho D_m C_p},$$

where λ represents the convective heat transfer coefficient, D_m represents the mixture-averaged diffusion coefficient, and C_p the specific heat capacity at constant pressure.

Definition 2.5.3. (Deborah number)

It is defined as the ratio of relaxation time to deformation time, It is denoted by γ. Mathematically

$$\gamma = \frac{\lambda U}{2x}.$$

Definition 2.5.4. (Skin friction coefficient)

Skin friction coefficient represents the value of friction which occurs when fluid moves across the surface. It is denoted by C_f. Mathematically

$$C_f = \frac{\tau_w}{\rho U_w^2},$$

where τ_w represents shear stress at the wall, ρ the density and U_w the free stream velcity.

Definition 2.5.5. (Reynolds number)

It is the dimensionless number. It is the ratio of the internal force to the viscous force and describes the degree of laminar or turbulent flow. It is denoted by Re. It can be written as

$$Re = \frac{\rho \mathbf{V} l}{\mu} = \frac{\mathbf{V} l}{\nu}$$

where $\mathbf{V}$ is the fluid velocity, l the characteritics length, ρ the fluid density, μ the dynamic viscosity and ν the kinematic viscosity of the fluid.

Definition 2.5.6. (Nusselt number)

It is defined as the ratio between transfer of heat by convection and heat transport by conduction in the direction normal to the boundary. Mathematically,

$$Nu_x = \frac{\text{convective heat transfer coefficient}}{\text{conductive heat transfer coefficient}}$$

$$Nu_x = \frac{h\nabla T/\kappa\nabla T}{L} = \quad \frac{hL}{\kappa},$$

where $h\nabla T$ represents heat transfer by convection, $\kappa\nabla T/L$ stands for heat transfer by conduction, h denotes the convective heat transfer, L represents characteristics length, and κ stands for the thermal conductivity of the fluid.

Definition 2.5.7. (Brownian diffusion coefficient)

Brownian diffusion occurs due to the continuous collision between the molecules and nanoparticles of the fluid. It is denoted by D_B and is given by

$$D_B = \frac{K_B T C_c}{3\Pi\mu dp},$$

where K_B, T, C_c, and μ represents Boltzmann constant, temperature, correction factor and viscosity respectively.

Definition 2.5.8. (Thermophoresis diffusion coefficient)

Thermophoresis diffusion occurs when particles diffuse due to the effect of temperature gradient. It is denoted by D_T and is given by

$$D_T = \frac{-\upsilon_{th} T}{\nu \nabla T},$$

where υ_{th}, T, ν, and ∇T denote the thermophoretic velocity, temperature, kinematic viscosity and temperature gradient respectively.

Definition 2.5.9. (Sherwood number)

It is the nondimensional quantity which shows the ratio of the mass transport by convection to the transfer of mass by diffusion. It is denoted by Sh. Mathematically

$$Sh_x = \frac{KL}{D},$$

where L denotes the characteristic length, D the mass diffusivity, and K denotes the coefficient of mass transfer.

2.6 Boundary layer flow

The layer of fluid adjacent to the solid surface is known as the boundary layer. In fluid mechanics, boundary layer flow plays a significant role. The basic idea of boundary layer was first introduced by Ludwig Prandlt ($1874 - 1953$). It can be divided into further categories presented below:

- Hydrodynamic (velocity) boundary layer.
- Thermal boundary layer.
- Concentration boundary layer.

Definition 2.6.1. (Hydrodynamic boundary layer)

A region of a fluid flow where the transition from zero velocity at the solid surface to the free stream velocity at some extent far from the solid surface in the direction normal to the flow takes place in a very thin layer known as hydrodynamic boundary layer.

Definition 2.6.2. (Thermal boundary layer)

It is an area of the liquid nearest to the solid surface, where the fluid temperature is directly influenced by the cooling or heating from the surface.

Definition 2.6.3. (Concentration boundary layer)

It is an area of the liquid nearest to the solid surface, where fluid concentration is directly influenced by the diffusion of mass at the surface.

Definition 2.6.4. (Magnetohydrodynamics)

The study of dynamics of electrically conducting fluids such as plasmas or electrolytes etc is known as magnetohydrodynamics. It is denoted by MHD.

2.7 Similarity transformation

Similarity transformation [34] is a mathematical technique that is applicable in some cases by which the PDEs of a problem are converted into ODEs. This technique reduces the number of independent variables of the problem. It can be stated in a way that it is a rule which combines the two independent variables to get a new variable.

2.8 Basic equations

2.8.1 Continuity equation

The law of conservation of mass states that "mass of fluid can neither be created nor be destroyed". Continuity equation is the mathematical expression which expresses the mass conservation law. Equation of continuity for compressible fluids, can be written as

$$\frac{\partial \rho}{\partial t} + \nabla.(\rho \mathbf{V}) = 0,$$

where ρ denotes fluid density. If fluid density is constant, the above equation is treated as equation of continuity for incompressible fluids. For incompressible fluids, the above equation becomes

$$\nabla.\mathbf{V} = 0.$$

2.8.2 Momentum equation

Each particle of fluid obeys Newton's second law of motion which is at rest or in steady state. This law implies that the combination of all applied exterior forces acting on the particles is equal to the time rate of change of momentum of the body. This law can be written in the vector notation as

$$\rho \frac{d\mathbf{V}}{dt} = \mathrm{div}T + \rho b.$$

For Navier-Stokes equation

$$T = -pI + \mu A_1,$$

where A_1 is the tensor and first time it was produced by Rivlin-Erickson.

$$A_1 = \mathrm{grad}\mathbf{V} + (\mathrm{grad}\mathbf{V})^t.$$

In the above equations, $\frac{d}{dt}$ denotes material time derivative or total derivative, ρ denotes density, $\mathbf{V}$ denotes the fluid velocity, Cauchy stress tensor is T, body forces is b, p denotes the pressure, and dynamic viscosity is μ. In the matrix form Cauchy stress tensor is written as:

$$T = \begin{pmatrix} \sigma_{xx} & \tau_{yx} & \tau_{zx} \\ \tau_{xy} & \sigma_{yy} & \tau_{zy} \\ \tau_{xz} & \tau_{yz} & \sigma_{zz} \end{pmatrix},$$

where σ_{xx}, σ_{yy}, and σ_{zz} are normal stresses, others are the shear stresses. For two-dimensional flow, we have,
$\mathbf{V} = [u(x, y, 0), v(x, y, 0), 0]$ and thus

$$\text{grad}\mathbf{V} = \begin{pmatrix} \frac{\partial u}{\partial x} & \frac{\partial u}{\partial y} & 0 \\ \frac{\partial v}{\partial x} & \frac{\partial v}{\partial y} & 0 \\ 0 & 0 & 0 \end{pmatrix}.$$

In component form

$$\frac{\partial u}{\partial t} + u\frac{\partial u}{\partial x} + v\frac{\partial v}{\partial y} = -\frac{1}{\rho}\frac{\partial p}{\partial y} + \nu\left(\frac{\partial^2 u}{\partial x^2} + \frac{\partial^2 u}{\partial y^2}\right),$$

Similarly, we write the Y and Z components respectively, as follows:

$$\frac{\partial v}{\partial t} + u\frac{\partial v}{\partial x} + v\frac{\partial v}{\partial y} = -\frac{1}{\rho}\frac{\partial p}{\partial y} + \nu\left(\frac{\partial^2 v}{\partial x^2} + \frac{\partial^2 v}{\partial y^2}\right),$$

$$\frac{\partial w}{\partial t} + u\frac{\partial w}{\partial x} + v\frac{\partial v}{\partial y} = -\frac{1}{\rho}\frac{\partial p}{\partial y} + \nu\left(\frac{\partial^2 w}{\partial x^2} + \frac{\partial^2 w}{\partial y^2}\right).$$

2.8.3 Energy equation

Energy equation is derived from the law of conservation of energy. According to this law, "energy can neither be created nor be destroyed". It may change from one form to another form in an isolated system. The total energy of the system is

conserved. Mathematically, it can be written as,

$$\rho C_p \frac{d\theta}{dt} = k\nabla^2\theta + \tau.L,$$

where ρ denotes the density, C_p represents the specific heat of the fluid at constant pressure, k denotes the thermal conductivity, while τ and θ denote the stress tensor and temperature, respectively.

2.9 Solution methodology

2.9.1. Shooting method

Consider the 2nd order two point boundary value problem (BVP):

$$y'' = f(x, y, y') \tag{2.1}$$

subjected to the boundary conditions:

$$y(0) = 0, \qquad y(A) = \alpha,$$

where α is some known constant. In order to apply the shooting method for the BVP (2.1), we first convert the Eq. (2.1) into a system of two first order ODEs. Using the notation, $y = y_1$, $y_1' = y_2$, we have

$$y_1' = y_2, \tag{2.2}$$

$$y_2' = f(x, y_1, y_2), \tag{2.3}$$

the associated boundary conditions reduced as:

$$y_1(0) = 0, \qquad y_1(A) = \alpha.$$

By considering $y_2(0)= s$, the first order system of Eqs. (2.2) and (2.3) together with $y_1(0)= 0$, $y_2(0)= s$ is an initial value problem (IVP) and can be solved by using the Runge-Kutta method of order four (RK-4). Then we get both y_1 and y_2 computed at the decided nodes. If $y_1(A)$ is sufficiently close to α, then this y_1 is an approximate solution, if not we have to choose another value of α and the process is repeated again. Newton method is used to refine the initial guess. This process is continued until a satisfactory accuracy is achieved. Its main advantage is its efficiency and fastness. If the solution is extremely sensitive to the assumed initial condition, then parallel shooting method is applied (see Na [35] for details).

Chapter 3

MHD melting heat transfer of Williamson nanofluid with the effect of chemical reaction

In this chapter, we perform the numerical investigation of MHD boundary layer flow and melting heat transfer of two-dimensional steady state flow of an incompressible Williamson nanofluid over a stretching surface in a porous medium. The modeled boundary layer equations for momentum, energy and concentration are obtained using the boundary layer approximations. By using an appropriate transformation, we convert the system of dimensional partial differential equations (nonlinear) into coupled dimensionless ordinary differential equations. A numerical technique based on the shooting method is applied for solution of the system of ODEs. The impact of physical parameters on dimensionless velocity, concentration, and temperature profiles is discussed through tables and graphs. In this chapter, review of the Krishnamurthy *et al.* [27] has been presented.

3.1 Problem formulation

Let us consider the numerical investigation of MHD boundary layer flow of an incompressible Williamson nanofluid. The flow is two-dimensional past a stretching surface with porous medium. Schematic diagram of the system under investigation is shown in the Figure 3.1. The plate has been stretched with velocity $u = ax$, $(a > 0)$ along x-direction. In addition, fluid is flowing in the presence of magnetic field. The magnetic field is supposed to be applied along the y-direction. The temperature at surface is T_w, U_w, C_w represent fluid velocity, nanoparticle concentration at surface respectively. Moreover, T_m denotes the melting surface temperature and T_∞ denotes the free stream temperature of the nanofluid. The free stream temperature T_∞ is greater than the melting surface temperature T_m. Here heat generation and viscous dissipation are cosidered to be negligibly small.

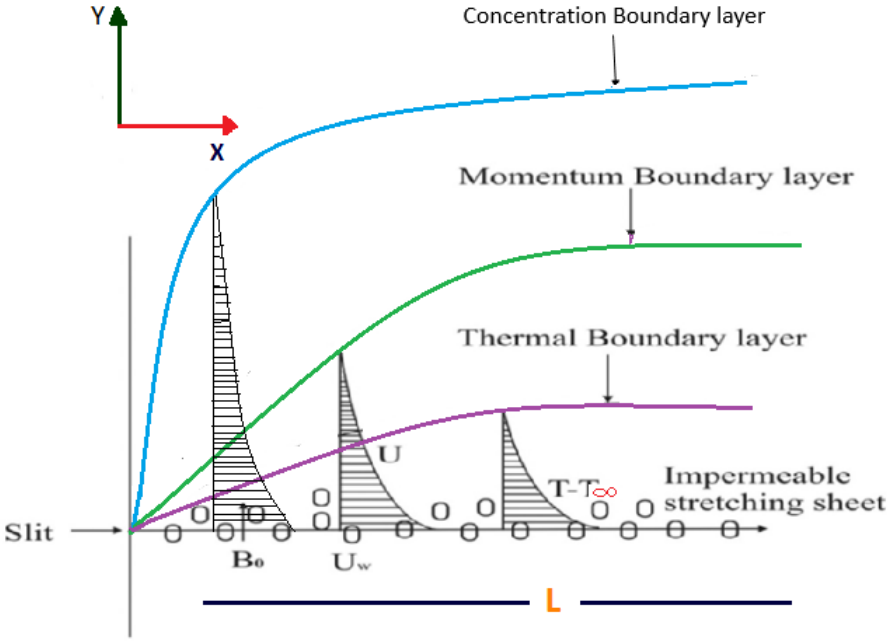

FIGURE 3.1: Geometry of the physical model.

The following system of equations are incorporated for mathematical model [27].
Continuity equation:

$$\frac{\partial u}{\partial x} + \frac{\partial v}{\partial y} = 0, \tag{3.1}$$

Momentum equation:

$$u\frac{\partial u}{\partial x}+v\frac{\partial u}{\partial y}=\nu\frac{\partial^2 u}{\partial y^2}+\sqrt{2}\nu\Gamma\frac{\partial u}{\partial y}\frac{\partial^2 u}{\partial y^2}-\sigma\frac{B_0^2}{\rho}u-\frac{\nu}{k'}u, \tag{3.2}$$

Energy equation:

$$u\frac{\partial T}{\partial x}+v\frac{\partial T}{\partial y}=\alpha_m\frac{\partial^2 T}{\partial y^2}+\tau\left[D_B\frac{\partial T}{\partial y}\frac{\partial C}{\partial y}+\frac{D_T}{T_\infty}\left(\frac{\partial T}{\partial y}\right)^2\right]-\frac{1}{(\rho c)_f}\frac{\partial q_r}{\partial y}, \tag{3.3}$$

Concentration equation:

$$u\frac{\partial C}{\partial x}+v\frac{\partial C}{\partial y}=D_B\frac{\partial^2 C}{\partial y^2}+\frac{D_T}{T_\infty}\frac{\partial^2 T}{\partial y^2}-k_0 C. \tag{3.4}$$

The associated boundary conditions for the modeled problem:

$$\left.\begin{aligned} &u=U_w(x)=ax, \quad T=T_m, \quad C=C_w, \qquad \text{as} \quad y=0,\\ &u=0, \quad T\to T_\infty, \quad C\to C_\infty, \quad \text{at} \quad y\to\infty,\\ &k\left(\frac{\partial T}{\partial y}\right)_{y=0}=\rho[\beta+c_s(T_m-T_0)]v(x,0), \end{aligned}\right\} \tag{3.5}$$

where u and v denote the components of fluid velocity along x and y direction, respectively, T denotes the temperature of the nanofluid, ρ the nanofluid density, α_m the thermal diffusivity of the nanofluid, ν the kinematic viscosity, D_B the coefficient of Brownian diffusion, D_T the coefficient of thermophoresis diffusion, k' the porous medium permeability, $(\rho c)_f$ the heat capacity of the fluid and $(\rho c)_p$ denotes the heat capacity of the nanoparticle. In the modeled problem, T_m denotes the temperature of melting surface, and T_∞ represents the temperature in the free-stream condition. Also, the radiative heat flux is given by:

$$q_r=\frac{-4\sigma^*}{3k^*}\frac{\partial T^4}{\partial y}, \tag{3.6}$$

where σ^* represents the Stefan- Boltzmann constant and k^* the coefficient of mean absorption. By applying Taylor series for temperature of free stream and ignoring

the terms of higher order, we have

$$T^4 = 4TT_\infty^3 - 3T_\infty^3. \tag{3.7}$$

Substituting Eqs. (3.6) and (3.7) in Eq. (3.3), we get

$$u\frac{\partial T}{\partial x} + v\frac{\partial T}{\partial y} = \alpha_m \frac{\partial^2 T}{\partial y^2} + \tau\left[D_B \frac{\partial T}{\partial y}\frac{\partial C}{\partial y} + \frac{D_T}{T_\infty}\left(\frac{\partial T}{\partial y}\right)^2\right] + \frac{16\sigma^* T_\infty^3}{3k^*(\rho c)_f}\frac{\partial^2 T}{\partial y^2}. \tag{3.8}$$

In order to obtain the solution of the problem, first of all the system of Eqs. (3.1), (3.2), (3.4) and (3.8) together with the boundary conditions (3.5) is converted into the dimensionless form by using suitable similarity transformation.

The following similarity transformation as defined in [27] has been used.

$$\xi = \sqrt{\frac{a}{\nu}}y, \qquad \theta(\xi) = \frac{T - T_m}{T_\infty - T_m}, \quad \phi(\xi) = \frac{C - C_w}{C_\infty - C_w}, \quad \psi = (a\nu)^{\frac{1}{2}} x f(\xi). \tag{3.9}$$

The continuity Eq. (3.1) is identically satisfied for the stream function $\psi = \psi(x, y)$. The velocity components are given by:

$$u = \frac{\partial \psi}{\partial y}, \qquad v = -\frac{\partial \psi}{\partial x}.$$

Using the similarity transformation from Eq. (3.9) in momentum Eq. (3.2), energy Eq. (3.3) and concentration Eq. (3.4) along the boundary conditions (3.5) we get the following system of ODEs:

$$f''' + ff'' - (f')^2 + \lambda f'' f''' - (Q + k_p)f' = 0, \tag{3.10}$$

$$\frac{1}{Pr}\left(1 + \frac{4}{3}R\right)\theta'' + f\theta' + Nb\phi'\theta' + Nt(\theta')^2 = 0, \tag{3.11}$$

$$\phi'' + Lef\phi' + \left(\frac{Nt}{Nb}\right)\theta'' - Le\gamma\phi = 0. \tag{3.12}$$

Here f, θ and ϕ are function of ξ and prime denotes derivative w.r.t ξ. The transformed BCs in the modeled problem are:

$$\left.\begin{array}{llll} f'(0)=1, & Prf(0)+M\theta'(0)=0, & \theta(0)=0, & \phi(0)=0, \\ f'(\xi)\to 0, & \theta(\xi)\to 1, & \phi(\xi)\to 1, & \text{as} \quad \xi\to\infty. \end{array}\right\} \tag{3.13}$$

The associated parameters appearing in the modeled problem are:

$Pr=\frac{\nu}{\alpha_m}=\frac{\mu C_p}{k}$, $R=\frac{4\sigma^* T_\infty^3}{kk^*}$, $k_p=\frac{\nu}{k'a}$, $\lambda=\gamma x\sqrt{\frac{2a^3}{\nu}}$, $\gamma=\frac{k_0U(C_\infty-C_w)}{\nu}$,
$Nt=\frac{\tau D_T(T_\infty-T_m)}{\nu T_\infty}$, $Q=\frac{\sigma B_0^2}{\rho a}$, $Le=\frac{\nu}{D_B}$, $Nb=\frac{\tau D_B(C_\infty-C_m)}{\nu}$,

where Pr denotes the Prandtl number, R the radiation parameter, k_p the permeability parameter, λ the non-Newtonian Williamson parameter, γ the chemical reaction parameter, Nt the thermophoresis parameter, Q the magnetic parameter, Nb the Brownian motion parameter and Le is the Lewis number.
The quantities of practical interest in this study are the Nusselt number (Nu_x), the skin friction coefficient (C_f), and the Sherwood number (Sh_x), respectively.

These are expressed as:

$$Nu_x=\frac{xq_w}{k(T_\infty-T_m)}, \quad C_f=\frac{\tau_w}{\rho U_w^2}, \quad \text{and } Sh_x=\frac{xq_m}{D_B(C_\infty-C_w)},$$

where τ_w is the shear stress, q_m the mass flux from the surface, and q_w the heat flux at the wall surface, given by:

$$q_m=-D_B\frac{\partial C}{\partial y}, \quad q_w=-k\frac{\partial T}{\partial y}, \quad \tau_w=\mu\left(\frac{\partial u}{\partial y}+\frac{\Gamma}{\sqrt{2}}\left(\frac{\partial u}{\partial y}\right)^2\right) \qquad \text{at} \quad y=0.$$

Using the dimensionless variables, we get

$$Nu_x(Re_x)^{\frac{1}{2}}=-\theta'(0), C_f(Re_x)^{\frac{1}{2}}=-f''(0)+\frac{\lambda}{2}f''(0)^2 \text{ and } Sh_x(Re_x)^{\frac{1}{2}}=-\phi'(0),$$

where Re_x denotes the Reynolds number and is expressed as:

$$Re_x=\frac{xU_w(x)}{v}.$$

3.2 Numerical solution

The analytical solution of the system of Eqs. (3.10)−(3.12) together with boundary conditions (3.13) can not be found because they are coupled and nonlinear in nature. These nonlinear coupled ODEs are solved numerically by the shooting technique. To apply this technique, we first convert the system of ODEs of higher order into the system of ODEs of first order. Eqs. (3.10) −(3.12) can be rewritten as,

$$
\begin{aligned}
f''' &= \frac{1}{1+\lambda f''}\left(-ff'' + (f')^2 + (Q+k_p)f'\right), \\
\theta'' &= \frac{3Pr}{3+4R}\left(-f\theta' - Nb\theta'\phi' - Nt(\theta')^2\right), \\
\phi'' &= -Lef\phi' - \left(\frac{Nt}{Nb}\right)\theta'' + Le\gamma\phi,
\end{aligned}
$$

subject to the boundary conditions:

$$
\begin{aligned}
&f'(0) = 1, \quad Prf(0) + M\theta'(0) = 0, \quad \theta(0) = 0, \quad \phi(0) = 0, \\
&f'(\xi) \to 0, \qquad \theta(\xi) \to 1, \qquad \phi(\xi) \to 1, \quad \text{as} \qquad \xi \to \infty.
\end{aligned}
$$

By using the following notations,

$$
f = y_1, \quad f' = y_2, \quad f'' = y_3, \quad \theta = y_4, \quad \theta' = y_5, \quad \phi = y_6, \quad \phi' = y_7,
$$

the system of first order ODEs are:

$$
\begin{aligned}
y_1' &= y_2, \\
y_2' &= y_3, \\
y_3' &= \frac{1}{1+\lambda y_3}\left(-y_1 y_3 + y_2^2 + (Q+k_p)y_2\right), \\
y_4' &= y_5, \\
y_5' &= \frac{3Pr}{3+4R}\left(-y_1 y_5 - Nb(y_5 y_7) - Nt(y_5)^2\right), \\
y_6' &= y_7, \\
y_7' &= -Le y_1 y_7 + Le\gamma y_6 - \frac{Nt}{Nb}\left(\frac{3Pr}{3+4R}\right)\left(-y_1 y_5 - Nb(y_5 y_7) - Nt(y_5^2)\right),
\end{aligned}
$$

subject to the following initial conditions:

$$
\begin{aligned}
y_1(0) &= \eta_1, \\
y_2(0) &= 1, \\
y_3(0) &= \eta_2, \\
y_4(0) &= 0, \\
y_5(0) &= -\frac{Pr\eta_1}{M}, \\
y_6(0) &= 0, \\
y_7(0) &= \eta_3.
\end{aligned}
$$

To solve the above system of equations, the unbounded domain $[0, \xi_\infty]$ is restricted to a bounded domain $[0, \xi_e]$, where ξ_e= 5. This is due to the fact that increasing the value of ξ_e beyond 5 gives negligible variation in the numerical results. In the modeled problem, η_1, η_2, and η_3 are initial guesses which are required to solve the above first order system of ordinary differential equations with fourth order Runge-Kutta method. Newton iterative scheme is used to refine those initial guesses. The iterative process is repeated untill the following criteria is met.

$$
\max\left\{|y_2(\xi_\infty) - 0|, \quad |y_4(\xi_\infty) - 1|, \quad |y_6(\xi_\infty) - 1|\right\} < \epsilon,
$$

where $\epsilon = 10^{-5}$ is the tolerance for the modeled problem.

3.3 Code validation

In Table 3.1, comparison of Nusselt number for different values of Pr is displayed. We compare the results obtained by the shooting method with those computed by the Matlab built-in function bvp4c and found both to be in excellent agreement. Furthermore, our findings are compared with the published work of Khan and Pop [36], Gorla and Sidawi [37], and Nadeem and Hussain [38], which show a good agreement of numerical results.

				Present study	
Pr	Ref. [36]	Ref. [37]	Ref. [38]	bvp4c	Shooting
0.07	0.066	0.066	0.066	0.06616	0.06616
0.20	0.169	0.169	0.169	0.16910	0.16910
0.70	0.454	0.454	0.454	0.45411	0.45411
2.0	0.911	0.911	0.911	0.91023	0.91023

TABLE 3.1: Numerical results of Nusselt number for various values of Prandtl number.

3.4 Results and discussion

The objective of this section is to analyze the numerical results displayed in the tabular and graphical form. The numerical influence of different parameters for example, Prandtl number (Pr), dimensionless melting parameter (M), Brownian motion parameter (Nb), thermophoresis parameter (Nt), radiation parameter (R), Lewis number (Le), magnetic parameter (Q), non-Newtonian Williamson parameter (λ), permeability parameter (k_p), and chemical reaction parameter (γ) on the velocity profile, temperature profile, and concentration profile are displayed graphically. The values of the skin friction coefficient (C_f), local Nusselt number (Nu_x),

and local Sherwood number (Sh_x) are presented in tables.

In Table 3.2, numerical analysis of physical parameters such as non-Newtonian Williamson parameter and dimensionless melting parameter and their influence on skin friction coefficient (C_f) is presented. From this table, it is noted that an increase in the non-Newtonian Williamson parameter and dimensionless melting parameter, the skin friction coefficient (C_f) decreases.

Table 3.3 shows the effect of different physical parameters for example, permeability parameter, dimensionless melting parameter, non-Newtonian Williamson parameter, chemical reaction parameter and their impact on the Nusselt number and Sherwood number. We compare the results obtained by the shooting method with Matlab built-in function bvp4c and found both to be in excellent agreement. From this table, we can see that by increasing the values of permeability parameter, dimensionless melting parameter, non-Newtonian Williamson parameter, chemical reaction parameter, Nusselt number and Sherwood number both are decreased.

λ	M=0.3	M=0.6	M=1.0	M=1.5	M=2
0.0	1.70978	1.66571	1.63308	1.60870	1.59262
0.05	1.68270	1.63955	1.60763	1.58379	1.56808
0.1	1.65384	1.61173	1.5806	1.55737	1.54206
0.15	1.62277	1.58185	1.55163	1.52910	1.51425
0.2	1.58884	1.54936	1.52022	1.49848	1.48416

TABLE 3.2: Numerical results of -$\sqrt{R_e}C_f$ for numerous values of M and λ.

				$-\theta'(0)$		$-\phi'(0)$	
k_p	M	λ	γ	bvp4c	Shooting	bvp4c	Shooting
0	0.5	0.2	0.01	2.1656	2.1656	0.3345	0.3345
1				1.9578	1.9578	0.2975	0.2975
2				1.7914	1.7914	0.2698	0.2698
	0.5			1.7914	1.7914	0.2698	0.2698
	1			1.1970	1.1970	0.0920	0.0920
	2			0.7392	0.7392	0.0139	0.0139
		0.01		1.8511	1.8511	0.2780	0.2780
		0.1		1.8256	1.8256	0.2744	0.2744
		0.2		1.7914	1.7914	0.2698	0.2698
			0.05	1.7661	1.7661	0.2725	0.2725
			0.1	1.7364	1.7364	0.2761	0.2761
			0.2	1.6832	1.6832	0.2841	0.2841

TABLE 3.3: Numerical results of Sherwood number $(-\phi'(0))$, and Nusselt number $(-\theta'(0))$ for different parameters.

The numerical results are presented for the physical interpretation of various values of relevant parameters in Figures 3.2−3.19.

Impact of melting parameter (M)

The influence of dimensionless melting parameter on velocity profile $f'(\xi)$ and dimensionless temperature profile $\theta(\xi)$ is shown in Figure 3.2 and 3.3 respectively. The graphical demonstration shows that for the increasing values of dimensionless melting parameter, the velocity profile and thickness of the boundary layer increases slightly and the temperature distribution decreases. It is found that an increase in the dimensionless melting parameter increases the melting intensity, which acts as boundary condition at the stretching surface and has a tendency to make the boundary layer thicker.

Impact of radiation parameter (R)

The influence of radiation parameter on profile of temperature distribution is displayed in Figure 3.4. From the figure it is observed that by increasing the radiation parameter, temperature profile decreases significantly. It is because of the fact that

the increasing values of radiation parameter lead to decrease the thickness of the boundary layer and enhance the heat transfer rate with chemical effect on the melting surface. Figure 3.5 represents that by increasing the radiation parameter, enhances the concentration profile $\phi(\xi)$.

Impact of Lewis number (Le)

The impact of Le on dimensionless temperature profile $\theta(\xi)$ can be seen as in Figures 3.6. From the figure, it is observed that by increasing values of Lewis number temperature near the surface of plate decreases and away from the surface of plate increases and concentration as well as the thickness of concentration increases. This is due to the fact that Le physically expresses the respective contribution of rate of thermal diffusion to the rate of species diffusion in the boundary layer regime. As increasing values of Lewis number reduce the thickness of thermal boundary layer and temperature decrease. It also reveals that the concentration gradient at surface of the plate increases.

Impact of magnetic parameter (Q)

Figures 3.8 and 3.9 demonstrate the influence of the magnetic parameter on the dimensionless profile of velocity distribution $f'(\xi)$ and dimensionless profile of temperature distribution $\theta(\xi)$, respectively. From these figures, it is clear that with increasing values of the magnetic parameter, profile of velocity decreases. It is also observed that temperature distribution $\theta(\xi)$ shows increasing effects as the magnetic parameter increases. The reason beyond this electrically conducting fluid produces a resistive force known as Lorentz force, which opposes the flow and has a tendency to make the fluid motion slow down in the boundary layer and therefore reduces the profile of velocity whereas its temperature $\theta(\xi)$ increases with the increase in magnetic parameter.

Impact of thermophoresis parameter (Nt)

The impact of thermophoresis parameter on the dimensionless profile of temperature distribution $\theta(\xi)$ and dimensionless profile of concentration distribution $\phi(\xi)$ are presented respectively in Figures 3.10 and 3.11. It is clear, from these figures profile of temperature and their associative thickness of thermal bondary layer of the thermal field increase with the increasing values of thermophoresis parameter. It is also noticed that for varying values of Nt concentration profile $\phi(\xi)$ and related thickness of bondary layer increases.

Impact of permeability parameter (k_p)

Figures 3.12 and 3.13 indicate the influence of the permeability parameter on the dimensionless profile of velocity distribution $f'(\xi)$ and dimensionless profile of the temperature produces a resistive force, that has a tendency to slow down the fluid motion. It is observed that resistance increases in the fluid motion by increasing values of the permeability parameter. Therefore, it is concluded that velocity profile $f'(\xi)$ decreases and temperature profile $\theta(\xi)$ increases by increasing values of permeability parameter.

Impact of non-Newtonian Williamson parameter (λ)

From Figures 3.14 and 3.15, we observe the effect of non-Newtonian Williamson parameter on the velocity and temperature profiles respectively. It is observed that the velocity profile and thickness of boundary layer decrease by increasing values of λ. It is also observed that the profile of temperature and thickness of thermal boundary layer decreases.

Impact of chemical reaction parameter (γ)

Figure 3.16 explains the influence of the chemical reaction parameter on the profile of concentration. It is noted that increasing values of chemical reaction parameter

concentration as well as the thickness of concentration decrease. It is because of the fact that the chemical reaction in this system results in chemical dissipation and therefore results in decrease in the profile of concentration. The most significant influence is that chemical reaction tends to decrease the overshoot in the concentration profiles and their associated boundary layer.

Impact of Prandtl number (Pr)

The impact of Pr on the profile of temperature field in the presence of melting parameter is displayed in Figure 3.17. From figure, we deduce that by increasing the values of Prandtl number, temperature profile increases. This is because the larger values of Prandtl number possess smaller thermal diffusivity and smaller Prandtl number have stronger thermal diffusivity. This change in thermal diffusivity produces a reduction in the temperature and thickness of thermal boundary layer.

Impact of Brownian motion parameter (Nb)

Figures 3.18 and 3.19 depict that by increasing Brownian motion parameter, temperature profile and thickness of boundary layer increases slightly whereas concentration profile decreases significcantly.

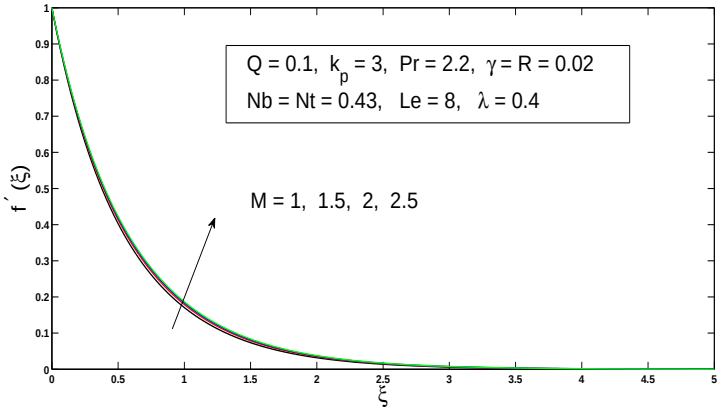

FIGURE 3.2: Impact of melting parameter on the velocity profile.

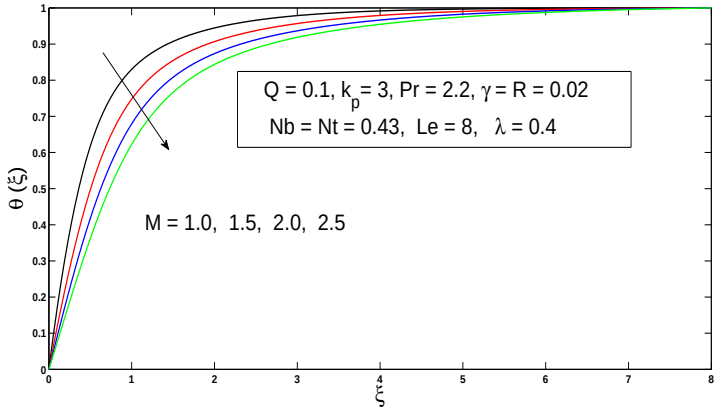

FIGURE 3.3: Influence of melting parameter on the temperature field.

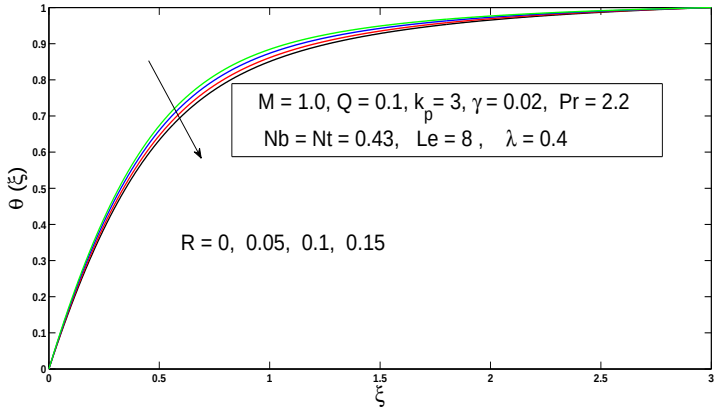

FIGURE 3.4: Effect of radiation parameter on the dimensionless temperature.

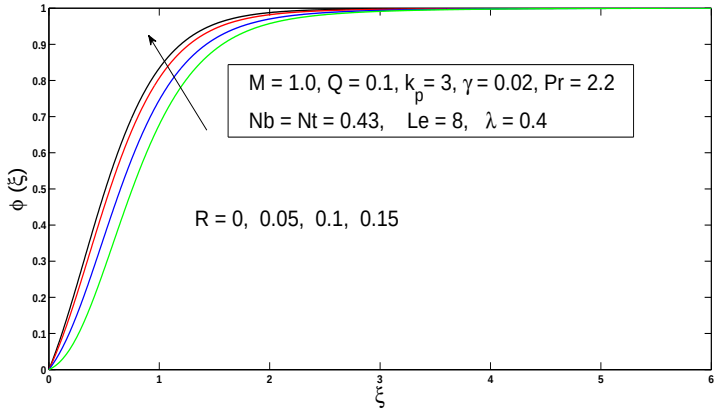

FIGURE 3.5: Effect of radiation parameter on the dimensionless concentration.

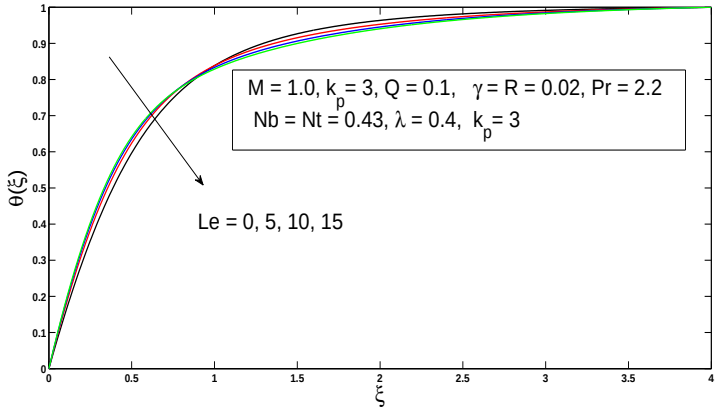

FIGURE 3.6: Imapct of Lewis number on the dimensionless temperature.

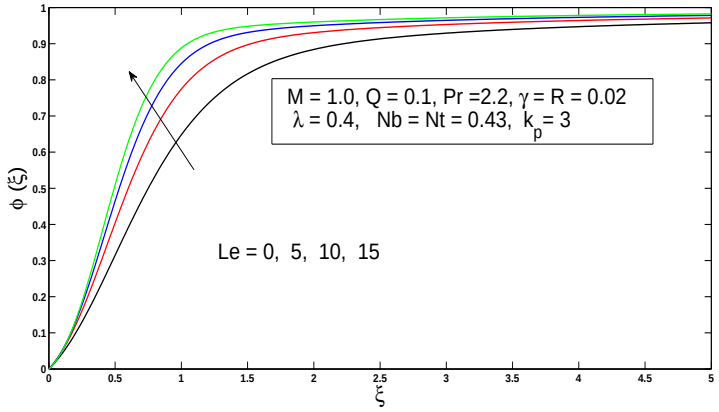

FIGURE 3.7: Imapct of Lewis number on the dimensionless concentration.

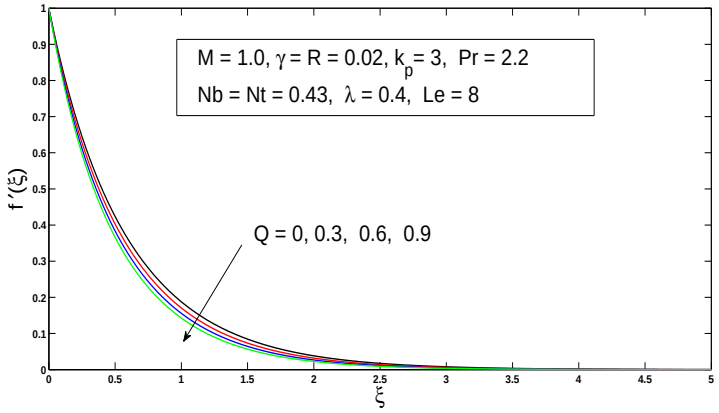

FIGURE 3.8: Impact of magnetic parameter on the velocity field.

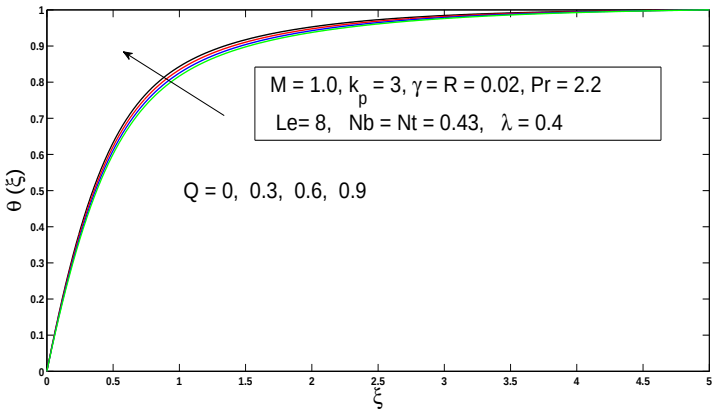

FIGURE 3.9: influence of magnetic parameter on the temperature profile.

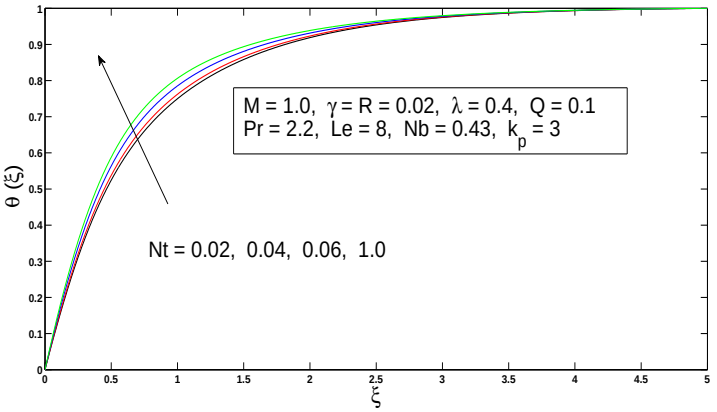

FIGURE 3.10: Effect of thermophoresis parameter on the dimensionless temperature.

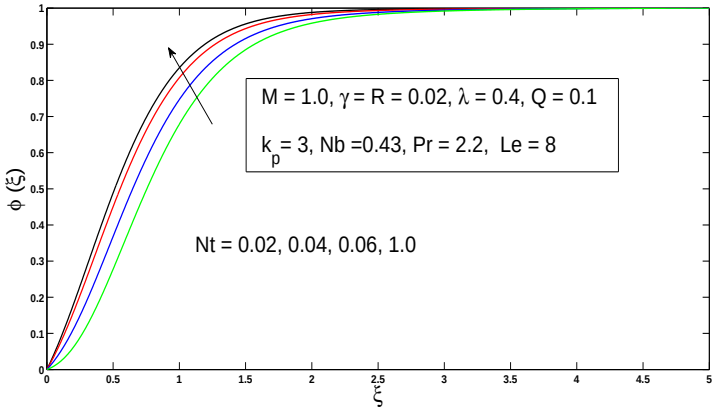

FIGURE 3.11: Effect of thermophoresis parameter on the dimensionless concentration.

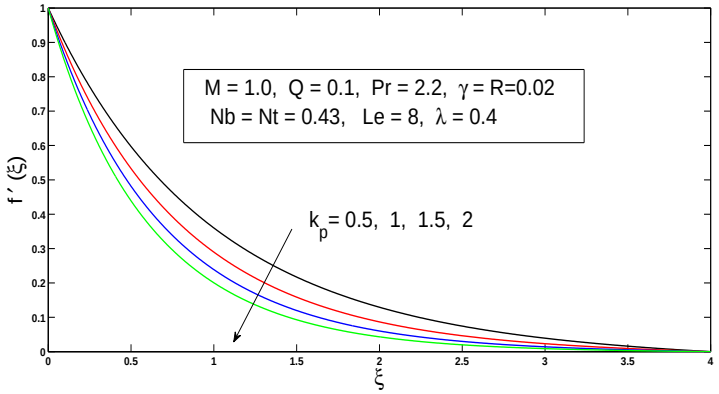

FIGURE 3.12: Effect of permeability parameter on the dimensionless velocity.

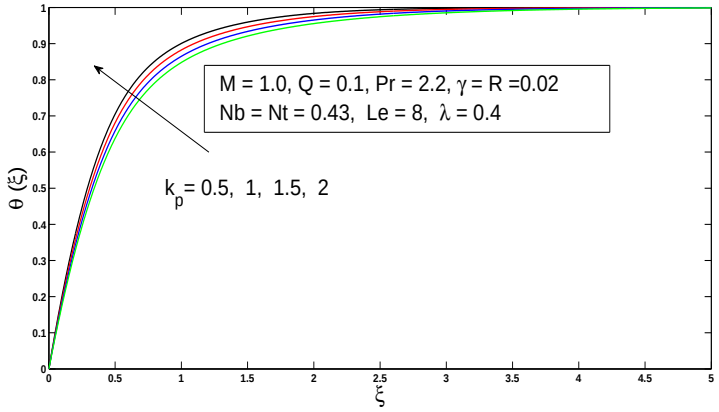

FIGURE 3.13: Effect of permeability parameter on the dimensionless temperature.

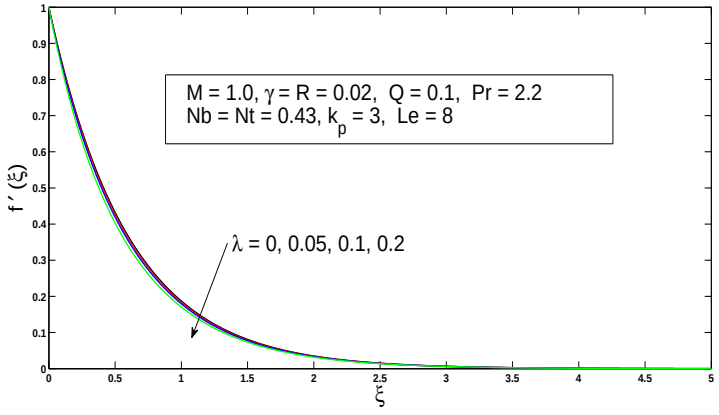

FIGURE 3.14: Effect of Williamson parameter on the dimensionless velocity.

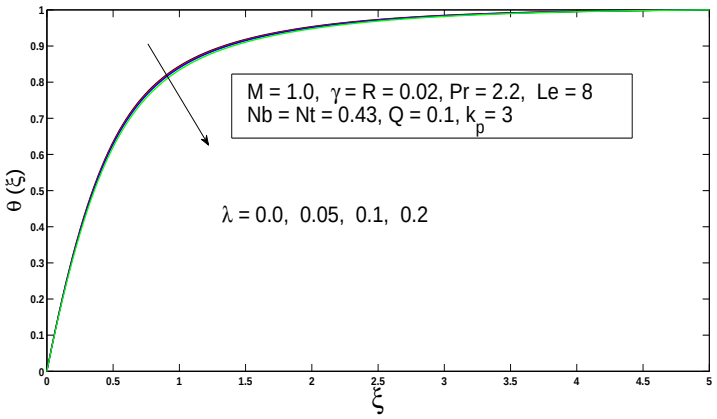

FIGURE 3.15: Effect of Williamson parameter on the dimensionless temperature.

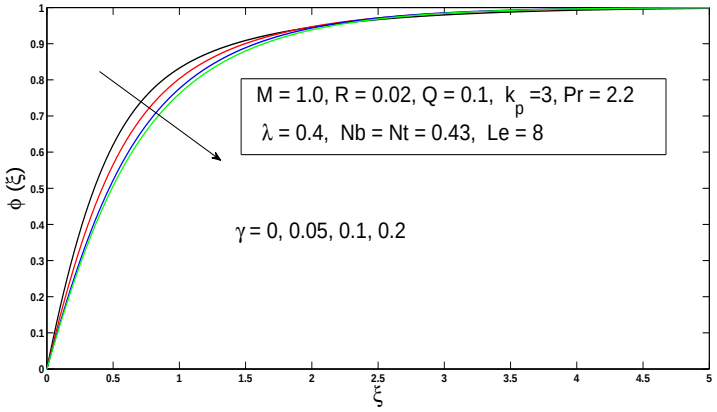

FIGURE 3.16: Influence of chemical reaction parameter on the dimensionless concentration.

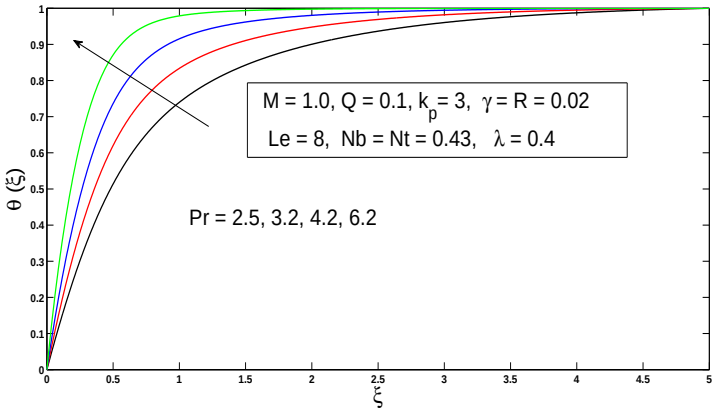

FIGURE 3.17: Influence of Pr on dimensionless temperature.

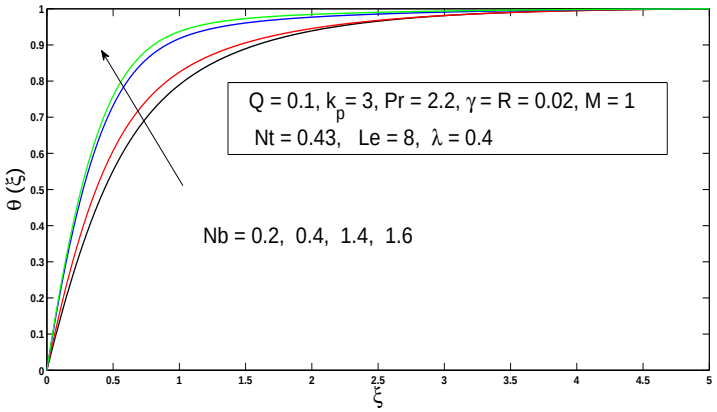

FIGURE 3.18: Influence of Brownian motion on the dimensionless temperature.

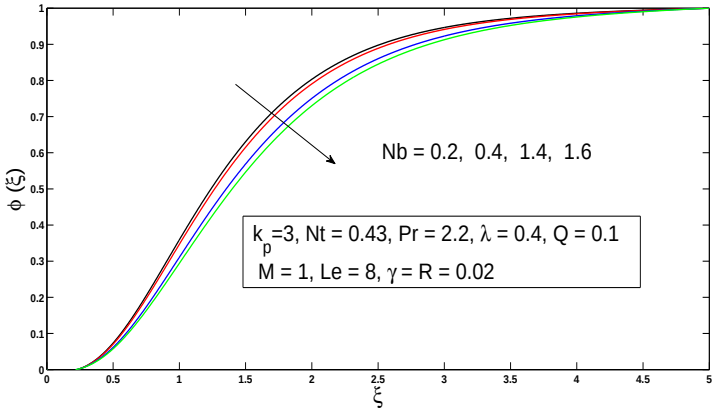

FIGURE 3.19: Impact of Brownian motion on the dimensionless concentration.

Chapter 4

Effect of Cattaneo-Christov heat flux on MHD Williamson nanofluid flow in a porous media

The main objective of this chapter is to extend the numerical investigation of MHD boundary layer flow and melting heat transfer of two-dimensional steady state flow of an incompressible Williamson nanofluid over a stretching surface in a porous medium with the effect of Cattaneo-Christov heat flux model. The inclusion of the physical effect in the energy equation make the problem more realistic and applicable in the industry. The nonlinear partial differential equations (PDEs) are converted into a system of ODEs (nonlinear) by using a suitable similarity transformations. The numerical solution of these modeled ordinary differential equations (ODEs) are achieved by utilizing shooting technique together with Runge-Kutta method of order four (RK-4). We also verify our results by using the Matlab function bvp4c. Finally the results are discussed for different parameters through graphs and tables.

4.1 Problem formulation

Let us consider the numerical investigation of MHD boundary layer flow of an incompressible Williamson nanofluid. The flow is two-dimensional past a stretching surface with porous medium. Schematic diagram of the system under investigation (see Figure 3.1). The plate has been stretched with velocity $u = ax$, $(a > 0)$ along x-axis. In addition, fluid is flowing in the presence of magnetic field. The magnetic field is supposed to be applied along the y-axis. The temperature at surface is T_w, U_w, C_w represent fluid velocity, nanoparticle concentration at surface respectively. Moreover, T_m denotes the melting surface temperature and T_∞ denotes the free stream temperature of the nanofluid. It is presumed that the free stream temperature T_∞ is greater than the melting surface temperature T_m. Here we can neglect heat generation and viscous dissipation under the mentioned presumption.

The following system of equations are incorporated for mathematical model[27, 39].
Continuity equation:

$$\frac{\partial u}{\partial x} + \frac{\partial v}{\partial y} = 0, \tag{4.1}$$

Momentum equation:

$$u\frac{\partial u}{\partial x} + v\frac{\partial u}{\partial y} = \nu\frac{\partial^2 u}{\partial y^2} + \sqrt{2}\nu\Gamma\frac{\partial u}{\partial y}\frac{\partial^2 u}{\partial y^2} - \sigma\frac{B_0^2}{\rho}u - \frac{\nu}{k'}u, \tag{4.2}$$

Energy equation:

$$\begin{aligned} u\frac{\partial T}{\partial x} + v\frac{\partial T}{\partial y} + \lambda_1 \left[\begin{array}{c} u\frac{\partial u}{\partial x}\frac{\partial T}{\partial x} + v\frac{\partial v}{\partial y}\frac{\partial T}{\partial y} + u\frac{\partial v}{\partial x}\frac{\partial T}{\partial y} + v\frac{\partial u}{\partial y}\frac{\partial T}{\partial x} \\ +2uv\frac{\partial^2 T}{\partial x \partial y} + u^2\frac{\partial^2 T}{\partial x^2} + v^2\frac{\partial^2 T}{\partial y^2} \end{array} \right] \\ = \alpha_m\frac{\partial^2 T}{\partial y^2} + \tau\left[D_B\frac{\partial T}{\partial y}\frac{\partial C}{\partial y} + \frac{D_T}{T_\infty}\left(\frac{\partial T}{\partial y}\right)^2 \right] - \frac{1}{(\rho c)_f}\frac{\partial q_r}{\partial y}, \end{aligned} \tag{4.3}$$

Concentration equation:

$$u\frac{\partial C}{\partial x} + v\frac{\partial C}{\partial y} = D_B\frac{\partial^2 C}{\partial y^2} + \frac{D_T}{T_\infty}\frac{\partial^2 T}{\partial y^2} - k_0 C. \tag{4.4}$$

The associated boundary conditions for the modeled problem:

$$\left.\begin{aligned} &u = U_w(x) = ax, \quad T = T_m, \quad C = C_w, \qquad \text{as} \quad y = 0, \\ &u = 0, \quad T \to T_\infty, \quad C \to C_\infty, \quad \text{at} \quad y \to \infty, \\ &k\left(\frac{\partial T}{\partial y}\right)_{y=0} = \rho[\beta + c_s(T_m - T_0)]v(x,0), \end{aligned}\right\} \tag{4.5}$$

Here u and v denote the velocity components in the x and y direction, respectively. T denotes the temperature of the nanofluid, ρ denotes the nanofluid density, α_m the thermal diffusivity of the nanofluid, ν the kinematic viscosity, D_B the Brownian diffusion coefficient, D_T the coefficient of thermophoresis diffusion, k' the porous medium permeability, $(\rho c)_f$ the heat capacity of the fluid, and $(\rho c)_p$ denotes the heat capacity of the nanoparticle. In the modeled problem T_m denotes the melting surface temperature, T_∞ represents the temperature in the free-stream condition, and λ_1 is the thermal relaxation time of heat flux.

In order to obtain the solution of the problem, first of all system of Eqs. (4.1)−(4.4) together with the boundary conditions (4.5) is converted into the dimensionless form by using suitable similarity transformation. The following similarity transformation as defined in [27] has been used.

$$\xi = \sqrt{\frac{a}{\nu}}y, \qquad \theta(\xi) = \frac{T - T_m}{T_\infty - T_m}, \quad \phi(\xi) = \frac{C - C_w}{C_\infty - C_w}, \quad \psi = (a\nu)^{\frac{1}{2}} x f(\xi). \tag{4.6}$$

The continuity Eq. (4.1) is identically satisfied for the stream function $\psi = \psi(x, y)$. The components of velocity are given by:

$$u = \frac{\partial \psi}{\partial y}, \qquad v = -\frac{\partial \psi}{\partial x}.$$

Using the similarity transformation from Eq. (4.6) in momentum Eq. (4.2), energy Eq. (4.1), and concentration Eq. (4.4) along the boundary conditions (4.5) we get

the following system of ODEs:

$$f''' + ff'' - (f')^2 + \lambda f''f''' - (Q + k_p)f' = 0, \tag{4.7}$$

$$\left(1 + \frac{4}{3}R - \gamma_1 Pr f^2\right)\theta'' + Pr\left(f\theta' + Nb\phi'\theta' + Nt(\theta')^2 - \gamma_1 ff'\theta'\right) = 0, \tag{4.8}$$

$$\phi'' + Lef\phi' + \left(\frac{Nt}{Nb}\right)\theta'' - Le\gamma\phi = 0. \tag{4.9}$$

Here f, θ and ϕ are function of ξ and prime denotes derivative w.r.t ξ. The transformed BCs in the modeled problem are:

$$\left.\begin{array}{llll} f'(0) = 1, & Prf(0) + M\theta'(0) = 0, & \theta(0) = 0, & \phi(0) = 0, \\ f'(\xi) \to 0, & \theta(\xi) \to 1, & \phi(\xi) \to 1, \text{as} & \xi \to \infty. \end{array}\right\} \tag{4.10}$$

The associated parameters appearing in the modeled problem are:

$$Pr = \frac{\nu}{\alpha_m} = \frac{\mu C_p}{k}, \quad R = \frac{4\sigma^* T_\infty^3}{kk^*}, \quad k_p = \frac{\nu}{k'a}, \quad \lambda = \gamma x\sqrt{\frac{2a^3}{\nu}}, \quad \gamma = \frac{k_0 U(C_\infty - C_w)}{\nu},$$
$$Nt = \frac{\tau D_T(T_\infty - T_m)}{\nu T_\infty}, \quad Q = \frac{\sigma B_0^2}{\rho a}, \quad Le = \frac{\nu}{D_B}, \quad \text{and} \quad Nb = \frac{\tau D_B(C_\infty - C_m)}{\nu},$$

where Pr denotes the Prandtl number, R the radiation parameter, k_p the permeability parameter, λ the non-Newtonian Williamson parameter, γ the chemical reaction parameter, Nt the thermophoresis parameter, Q the magnetic parameter, Nb the Brownian motion parameter, and Le the Lewis number.

The quantities of practical interest in this study are the Nusselt number (Nu_x), the Sherwood number (Sh_x), and the skin friction coefficient (C_f), respectively. These are defined as:

$$Sh_x = \frac{xq_m}{D_B(C_\infty - C_w)}, Nu_x = \frac{xq_w}{k(T_\infty - T_m)} \text{ and } C_f = \frac{\tau_w}{\rho U_w^2},$$

where τ_w is the shear stress, q_m the mass flux from the surface, and q_w the heat flux at the wall surface, given by:

$$q_m = -D_B\frac{\partial C}{\partial y}, \quad q_w = -k\frac{\partial T}{\partial y}, \quad \tau_w = \mu\left(\frac{\partial u}{\partial y} + \frac{\Gamma}{\sqrt{2}}\left(\frac{\partial u}{\partial y}\right)^2\right) \quad \text{at} \quad y = 0.$$

Using the dimensionless variables, we get

$$Nu_x(Re_x)^{\frac{1}{2}} = -\theta'(0),\ C_f(Re_x)^{\frac{1}{2}} = -f''(0) + \frac{\lambda}{2}f''(0)^2 \ \text{ and } Sh_x(Re_x)^{\frac{1}{2}} = -\phi'(0),$$

where Re_x represents the Reynolds number and is defined as:

$$Re_x = \frac{xU_w(x)}{v}.$$

4.2 Numerical solution

The analytical solution of the system of Eqs. (4.7)−(4.9) together with boundary conditions (4.5) can not be found because they are coupled and nonlinear in nature. These nonlinear coupled ODEs are solved numerically by the shooting technique. To apply this technique, we first convert the system of ODEs of higher order into the system of ODEs of first order. Eqs. (4.7)−(4.9) can be rewritten as,

$$\begin{aligned}
f''' &= \frac{1}{1+\lambda f''}\left(-ff'' + (f')^2 + (Q+k_p)f'\right),\\
\theta'' &= \left(\frac{-Pr}{1+\frac{4}{3}R - \gamma_1 Prf^2}\right)[f\theta' + Nb\theta'\phi' + Nt\theta'^2 - \gamma_1 ff'\theta'],\\
\phi'' &= -Lef\phi' - \left(\frac{Nt}{Nb}\right)\theta'' + Le\gamma\phi.
\end{aligned}$$

the associated boundary conditions are:

$$\begin{aligned}
&f'(0) = 1, \quad Prf(0) + M\theta'(0) = 0, \quad \theta(0) = 0, \quad \phi(0) = 0,\\
&f'(\xi) \to 0, \qquad \theta(\xi) \to 1, \qquad \phi(\xi) \to 1, \quad \text{as} \qquad \xi \to \infty.
\end{aligned}$$

By using the following notations,

$$f = y_1, \quad f' = y_2, \quad f'' = y_3, \quad \theta = y_4, \theta' = y_5, \quad \phi = y_6, \quad \phi' = y_7,$$

the system of first order ODEs are:

$$
\begin{aligned}
y_1' &= y_2, \\
y_2' &= y_3, \\
y_3' &= \frac{1}{1+\lambda y_3}\left(-y_1 y_3 + y_2^2 + (Q+k_p)y_2\right), \\
y_4' &= y_5, \\
y_5' &= \frac{-Pr\left[y_1 y_5 + Nb y_5 y_7 + Nt y_5^2 - \gamma_1 y_1 y_2 y_5\right]}{1+\frac{4}{3}R - \gamma_1 Pr y_1^2}, \\
y_6' &= y_7, \\
y_7' &= -Le y_1 y_7 + Le\gamma y_6 - \frac{Nt}{Nb}\left(\frac{3Pr}{3+4R}\right)\left(-y_1 y_5 - Nb(y_5 y_7) - Nt(y_5^2)\right),
\end{aligned}
$$

subject to the following initial conditions:

$$
\begin{aligned}
y_1(0) &= \eta_1, \\
y_2(0) &= 1, \\
y_3(0) &= \eta_2, \\
y_4(0) &= 0, \\
y_5(0) &= -\frac{Pr\eta_1}{M}, \\
y_6(0) &= 0, \\
y_7(0) &= \eta_3.
\end{aligned}
$$

To solve the above system of equations the unbounded domain $[0, \xi_\infty]$ is restricted to a bounded domain $[0, \xi_e]$, where ξ_e= 5. This is due to the fact that increasing the value of ξ_e beyond 5 gives negligible variation in the numerical result. In the modeled problem, η_1, η_2, and η_3 are initial guesses which are required to solve the above first order system of ordinary differential equations with fourth order Runge-Kutta method. Newton iterative scheme is used to refine those initial guesses. The iterative process is repeated untill the following criteria is met.

$$
\max\left\{|y_2(\xi_\infty) - 0|, \quad |y_4(\xi_\infty) - 1|, \quad |y_6(\xi_\infty) - 1|\right\} < \epsilon,
$$

where $\epsilon = 10^{-5}$ is the tolerance for the modeled problem.

4.3 Results and discussion

The objective of this section is to analyze numerical results displayed in the tabular and graphical form. The numerical influence of different parameters for example, Prandtl number (Pr), dimensionless melting parameter (M), Brownian motion parameter (Nb), thermophoresis parameter (Nt), radiation parameter (R), Lewis number (Le), magnetic parameter (Q), permeability parameter (k_p), and chemical reaction parameter (γ), on the velocity, temperature, and concentration profiles are displayed graphically. Numerical values of the local Nusselt number, and local Sherwood number are presented in table.

Table 4.1 shows the effect of various parameters on local Nusselt number and local Sherwood number are of great interest for engineers. In table 4.1 the numerical analysis of different physical parameters such as permeability parameter, melting parameter, Non-Newtonian Williamson parameter, chemical reaction parameter, and Deborah number and their impacts on the local Nusselt number and local Sherwood number. We compare the results obtained by the shooting method with Matlab built-in function bvp4c and found both to be in excellent agreement. From this table, we can see that by increasing the values of Permeability parameter, dimensionless melting parameter, non-Newtonian Williamson parameter, chemical reaction parameter, and Deborah number Nusselt number and Sherwood number both are decreased.

					$-\theta'(0)$		$-\phi'(0)$	
k_p	M	λ	γ	γ_1	bvp4c	Shooting	bvp4c	Shooting
0	0.5	0.2	0.01	0.01	1.9617	l.9617	0.3498	0.3498
1					1.8626	1.8625	0.3117	0.3117
2					1.7960	1.7960	0.2829	0.2829
	0.5				1.7960	1.7960	0.2829	0.2829
	1				1.7813	1.7813	0.2488	0.248
	2				1.7511	0.7511	0.2392	0.2392
		0.01			1.7156	1.7156	0.2144	0.2144
		0.1			1.6553	1.6553	0.2077	0.2077
		0.2			1.6271	1.6271	0.1719	0.1719
			0.05		1.6163	1.6163	0.1631	0.1631
			0.1		1.6030	1.6030	0.1492	0.1492
			0.2		1.5830	1.5830	0.1292	0.1292
				0.02	1.5528	1.5528	0.0835	0.0835
				0.03	1.4935	1.4935	0.0437	0.0437
				0.04	1.4542	1.4542	0.0239	0.0239

TABLE 4.1: Numerical results of Sherwood number $(-\phi'(0))$, and Nusselt number $(-\theta'(0))$ for various parameters.

The numerical results are presented for the physical interpretation of various values of relevant parameters in Figures 4.1−4.9.

Impact of melting parameter (M)

The impact of non-dimensional melting parameter on velocity profile $f'(\xi)$ and non-dimensional temperature profile $\theta(\xi)$ is shown in Figure 4.1 and 4.2 respectively. The graphical demonstration shows that for the increasing values of non-dimensional melting parameter, the velocity profile and thickness of the boundary layer increases slightly and the temperature distribution decreases. It is found that an increase in the non-dimensional melting parameter increases the melting intensity, which acts as boundary condition at the stretching surface and has a tendency to make the boundary layer thicker.

Impact of radiation parameter (R)

The effect of radiation parameter on profile of temperature distribution is displayed in Figure 4.3. From the figure it is observed that by increasing the radiation parameter, temperature profile decreases significantly. It is because of the fact that the increasing values of the radiation parameter lead to decrease the thickness of the boundary layer and enhance the heat transfer rate with chemical effect on the melting surface. Figure 4.4 represents that increasing the radiation parameter, enhances the concentration profile $\phi(\xi)$.

Impact of Prandtl number (Pr)

The influence of Pr on the profile of temperature field in the presence of melting parameter is displayed in Figure 4.5. From figure, we deduce that by increasing the values of Prandtl number, temperature profile increases. This is because the larger values of Prandtl number possess smaller thermal diffusivity and smaller Prandtl number have stronger thermal diffusivity. This change in thermal diffusivity produces a reduction in the temperature and thickness of thermal boundary layer.

Impact of Brownian motion parameter (Nb)

Figures 4.6 and 4.7 depict that by increasing Brownian motion parameter, temperature profile and thickness of boundary layer increases slightly whereas concentration profile decreases significcantly.

Impact of permeability parameter (k_p)

Figures 4.8 and 4.9 indicate the influence of the permeability parameter on the non-dimensional profile of velocity distribution $f'(\xi)$ and non-dimensional profile of the temperature produces a resistive force, that has a tendency to slow down the fluid motion. It is observed that resistance increases in the fluid motion by

increasing the values of the permeability parameter. Therefore, it is concluded that the velocity profile $f'(\xi)$ decreases and temperature profile $\theta(\xi)$ increases by increasing values of permeability parameter.

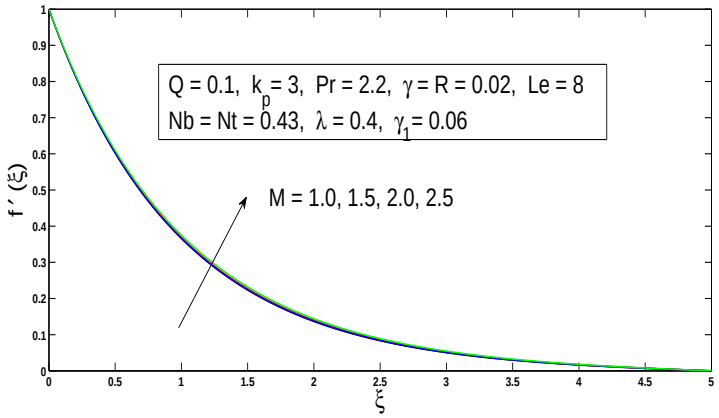

FIGURE 4.1: Impact of melting parameter on the dimensionless velocity.

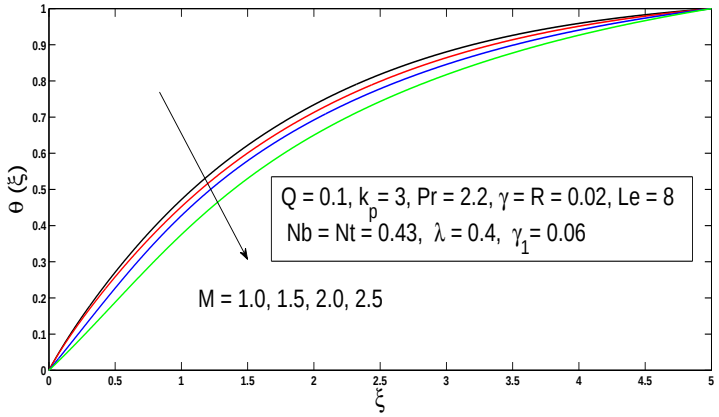

FIGURE 4.2: Impact of melting parameter on the dimensionless temperature.

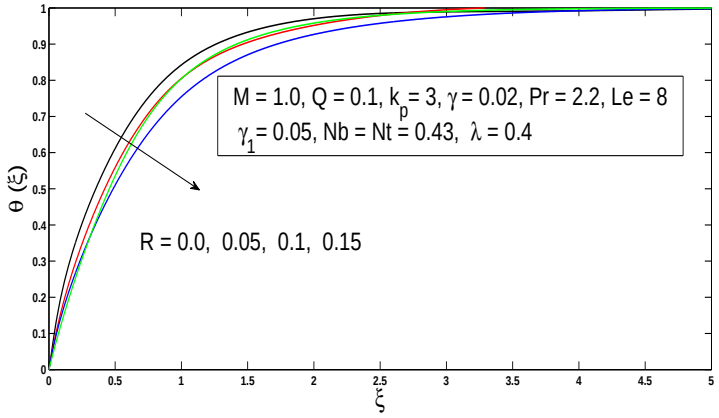

FIGURE 4.3: Effect of radiation parameter on the dimensionless temperature.

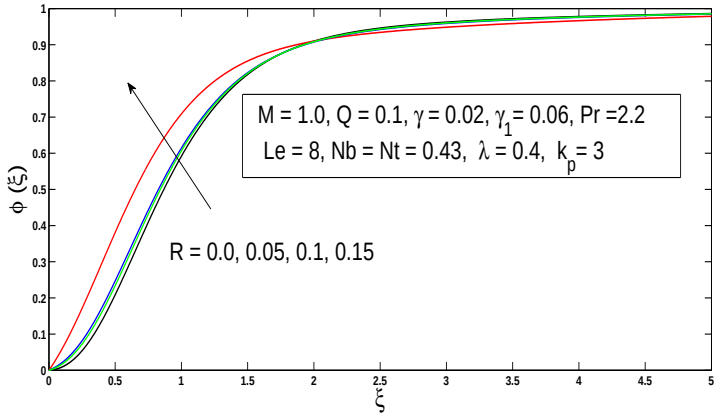

FIGURE 4.4: Effect of radiation parameter on the dimensionless concentration.

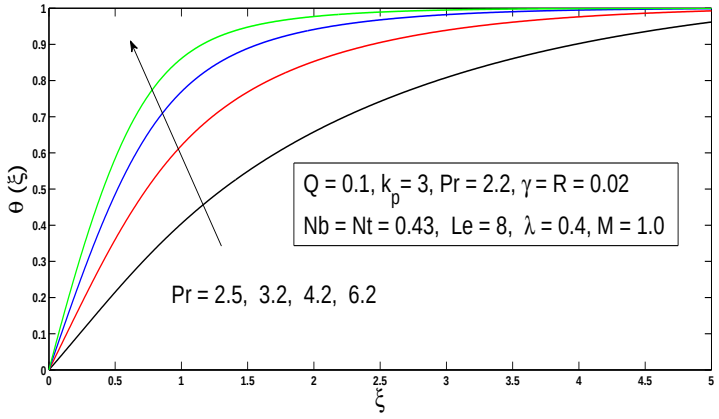

FIGURE 4.5: Effect of Prandtl number on the dimensionless temperature.

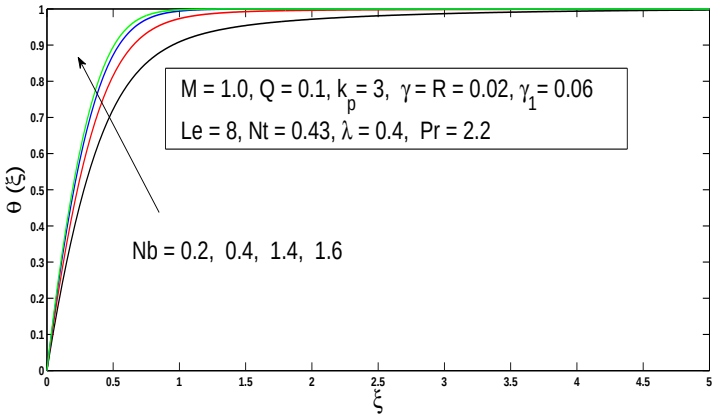

FIGURE 4.6: Effect of Brownian motion parameter on $\theta(\xi)$.

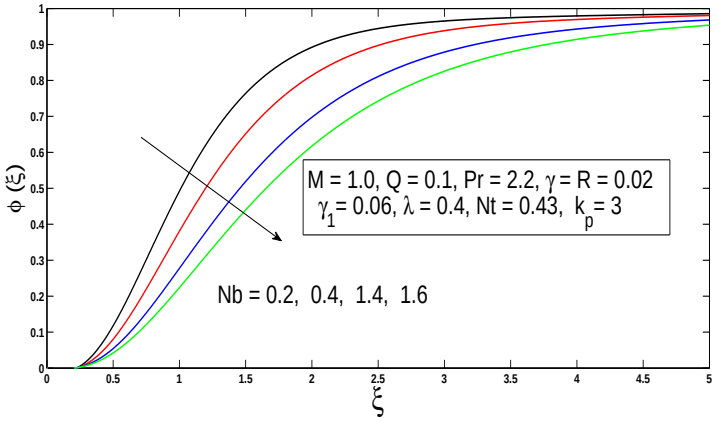

FIGURE 4.7: Behavior of Brownian motion parameter on the dimensionless concentration.

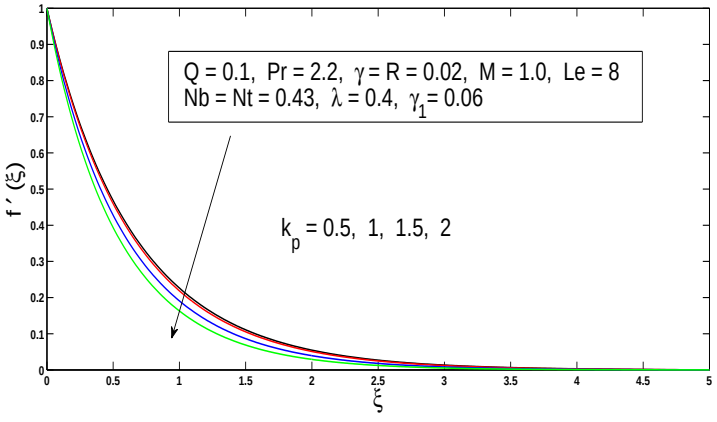

FIGURE 4.8: Effect of k_p on the dimensionless velocity.

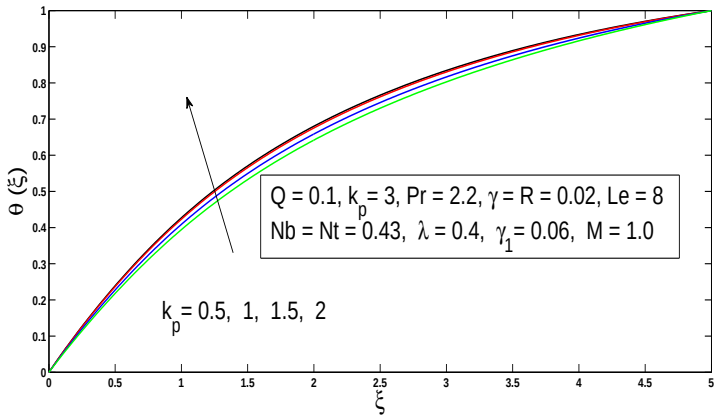

FIGURE 4.9: Representation of temperature profile for various values of k_p.

Chapter 5

Conclusion and outlook

In this dissertation, the analysis of MHD boundary layer flow and melting transfer of heat of two-dimensional steady state flow of an incompressible Williamson nanofluid on a stretching surface in a porous medium with the influence of magnetic field is investigated. Furthermore, the impact of heat flux model of Cattaneo-Christov is under consideration. The solution of the problem is obtained by converting governing PDEs into a system of ODEs utilizing similarity transformation and then numerically solving by applying the shooting technique. The numerical results are in good agreement with Matlab built-in function bvp4c solver. Physical significance of different parameters are discussed with respect to dimensionless velocity, temperature and concentrations profiles. From the figures the following conclusions have been drawn.

- Due to an increase in the magnetic parameter, the velocity profile increases and the temperature profile decreases.
- Due to an increase in the radiation parameter, the temperature field decreases whereas the concentration profile increases.
- The temperature profile increases with the increase of Pr.

- For increasing values of the magnetic parameter, the magnetic parameter has decreasing effects on the velocity profile, and increasing effects on the temperature θ.
- An increase in Brownian motion parameter, temperature profile increases, while the concentration profile decreases in the horizontal direction.
- Velocity field f' decreases by enlarging permeability parameter k_p.
- Temperature field θ decreases with an increase in permeability parameter k_p.
- Temperature field θ decreases for increasing values of γ_1.
- An increase in the values of non-Newtonian Williamson parameter causes decrease in the velocity profile and similar effects on temperature.
- By increasing the thermophoresis parameter Nt, momentum boundary layer thickness and concentration boundary layer thickness increases.
- For increasing values of non-Newtonian Williamson parameter, and melting parameter, the skin friction coefficient decreases.

5.1 Future recommendations

In future, this problem may be extended in many directions considering the following ideas:

- The impact of Joule heating.
- The impact of different nanoparticles.
- The impact of source and sink.
- The impact of viscous dissipation.

Bibliography

[1] G. B. Meir, "Basic of fluid mechanics," *M. Genick. Chicago*, 2013.

[2] B. Sakiadis, "Boundary layer behavior on continuous solid surfaces," *J. AIChE*, vol. 7, no. 1, pp. 26–28, 1961.

[3] L. Crane, "Flow past a stretching plate," *Zeitschrift für angewandte Mathematik und Physik*, vol. 21, no. 4, pp. 645–647, 1970.

[4] S. Shehzad, Z. Abdullah, F. Abbasi, T. Hayat, and A. Alsaedi, "Magnetic field effect in three-dimensional flow of an oldroyd-B nanofluid over a radiative surface," *J. Magn. Magn. Mater*, vol. 399, pp. 97–108, 2016.

[5] L. Zheng, J. Niu, X. Zhang, and L. Ma, "Dual solutions for flow and radiative heat transfer of a micropolar fluid over stretching/shrinking sheet," *Int. J. Heat Mass Transf.*, vol. 55, no. 25, pp. 7577–7586, 2012.

[6] B. Gireesha, A. Chamkha, S. Manjunatha, and C. Bagewadi, "Mixed convective flow of a dusty fluid over a vertical stretching sheet with non-uniform heat source/sink and radiation," *Int. J. Num. Meth. Heat Fluid Flow*, vol. 23, no. 4, pp. 598–612, 2013.

[7] E. Elbashbeshy, "Heat transfer over an exponentially stretching continuous surface with suction," *Arch. Mech.*, vol. 53, no. 6, pp. 643–651, 2001.

[8] E. Sanjayanand and K. Khan, "On heat and mass transfer in a viscoelastic boundary layer flow over an exponentially stretching sheet," *Int. J. Therm. Sci.*, vol. 45, no. 8, pp. 819–828, 2006.

[9] E. Magyari and B. Keller, "Heat and mass transfer in the boundary layers on an exponentially stretching continuous surface," *J. Phys.*, vol. 32, no. 5, pp. 577–585, 1999.

[10] S. U. S. Choi, "Enhancing thermal conductivity of fluids with nanoparticles," *Int. Meh. Eng.*, vol. 66, pp. 99–105, 1995.

[11] S. U. S. Choi, Z. Zhang, F. Yu, W. Lockwood, and E. Grulke, "Anomalous thermal conductivity enhancement in nanotube suspensions," *Appl. Phys. Lett.*, vol. 79, no. 14, pp. 2252–2254, 2001.

[12] K. Khanafer, K. Vafai, and M. Lightstone, "Buoyancy-driven heat transfer enhancement in a two-dimensional enclosure utilizing nanofluids," *Int. J. Heat Mass Transf.*, vol. 46, no. 19, pp. 3639–3653, 2003.

[13] H. Alfvén, "Existence of electromagnetic-hydrodynamic waves," *Nature*, vol. 150, no. 3805, pp. 405–406, 1942.

[14] I. Mbeledogu and A. Ogulu, "Heat and mass transfer of an unsteady MHD natural convection flow of a rotating fluid past a vertical porous flat plate in the presence of radiative heat transfer," *Int. J. Heat Mass Transf.*, vol. 50, no. 9, pp. 1902–1908, 2007.

[15] P. Kesavaiah, D. C. Satyanarayana and S. Venkataramana, "Effects of the chemical reaction and radiation absorption on an unsteady MHD convective heat and mass transfer flow past a semi-infinite vertical permeable moving plate embedded in a porous medium with heat source and suction," *Int. J. Appl. Math. Mech.*, vol. 7, no. 1, pp. 52–69, 2011.

[16] T. Hayat, S. Asad, M. Mustafa, and A. Alsaedi, "MHD stagnation-point flow of Jeffrey fluid over a convectively heated stretching sheet," *Comput. Fluids*, vol. 108, pp. 179–185, 2015.

[17] M. Mustafa, J. Khan, T. Hayat, and A. Alsaedi, "Sakiadis flow of Maxwell fluid considering magnetic field and convective boundary conditions," *AIP Adv.*, vol. 5, no. 2, p. 027106, 2015.

[18] N. Hari, M. Sivasankaran, S. Bhuvaneswari, and Z. Siri, "Effects of chemical reaction on MHD mixed convection stagnation point flow toward a vertical plate in a porous medium with radiation and heat generation," *J. Phys.*, vol. 662, no. 1, p. 012014, 2015.

[19] R. V. Williamson, "The flow of pseudoplastic materials," *Ind. Eng. Ch.*, vol. 21, no. 11, pp. 1108–1111, 1929.

[20] S. Nadeem, S. Hussain, and C. Lee, "Flow of a Williamson fluid over a stretching sheet," *Braz. J. Chem. Eng.*, vol. 30, no. 3, pp. 619–625, 2013.

[21] S. Nadeem and S. Hussain, "Flow and heat transfer analysis of Williamson nanofluid," *Appl. Nanosci.*, vol. 4, no. 8, pp. 1005–1012, 2014.

[22] T. Hayat and S. Hina, "Effects of heat and mass transfer on peristaltic flow of Williamson fluid in a non-uniform channel with slip conditions," *Int. J. Num. Methods in Fluids*, vol. 67, no. 11, pp. 1590–1604, 2011.

[23] T. Hayat, F. Abbasi, A. Alsaedi, and F. Alsaadi, "Hall and Ohmic heating effects on the peristaltic transport of a Carreau–Yasuda fluid in an asymmetric channel," *Z. Naturforsch*, vol. 68, pp. 43–51, 2014.

[24] T. Sarpakaya, "Flow of non-newtonian fluids in a magnetic field," *J. AIChE*, vol. 7, no. 2, pp. 324–328, 1961.

[25] V. Kumaran and G. Ramanaiah, "A note on the flow over a stretching sheet," *Acta Mecca*, vol. 116, no. 1, pp. 229–233, 1996.

[26] M. Qasim, "Heat and mass transfer in a Jeffrey fluid over a stretching sheet with heat source/sink," *Alex. Eng. J.*, vol. 52, no. 4, pp. 571–575, 2013.

[27] M. Krishnamurthy, B. Prasannakumara, B. Gireesha, and R. Gorla, "Effect of chemical reaction on MHD boundary layer flow and melting heat transfer of Williamson nanofluid in porous medium," *Eng. Sci. Technol. Int. J.*, vol. 19, no. 1, pp. 53–61, 2016.

[28] J. Fourier, "The analytic theory of heat," *Eng.Trans.*, 1822.

[29] C. Cattaneo, "Sulla conduzione del calore," *Atti Sem. Mat. Fis. Univ. Modena*, vol. 3:3, pp. 83–101, 1948.

[30] C. I. Christov, "On frame indifferent formulation of the Maxwell–Cattaneo model of finite-speed heat conduction," *Mech. Res. Commun.*, vol. 36, no. 4, pp. 481–486, 2009.

[31] M. Ostoja-Starzewski, "A derivation of the Maxwell–Cattaneo equation from the free energy and dissipation potentials," *Int. J. Eng. Sci.*, vol. 47, no. 7, pp. 807–810, 2009.

[32] V. Tibullo and V. Zampoli, "A uniqueness result for the Cattaneo–Christov heat conduction model applied to incompressible fluids," *Mech. Res. Commun.*, vol. 38, no. 1, pp. 77–79, 2011.

[33] J. A. Khan, M. Mustafa, T. Hayat, and A. Alsaedi, "Numerical study of Cattaneo-Christov heat flux model for viscoelastic flow due to an exponentially stretching surface," *PLOS one*, vol. 10, no. 9, p. e0137363, 2015.

[34] L. Cao, X. Si, and L. Zheng, "Convection of Maxwell fluid over stretching porous surface with heat source/sink in presence of nanoparticles: Lie group analysis." *Appl. Math. Mech.*, vol. 37, no. 4, pp. 433–442, 1961.

[35] T. Y. Na, "Computational methods in engineering boundary value problems," *Academic Press*, vol. 145, 1980.

[36] W. Khan and I. Pop, "Boundary-layer flow of a nanofluid past a stretching sheet," *Int.J. Heat Mass Transf.*, vol. 53, no. 11, pp. 2477–2483, 2010.

[37] R. S. R. Gorla and I. Sidawi, "Free convection on a vertical stretching surface with suction and blowing," *Appl. Sci. Res.*, vol. 52, no. 3, pp. 247–257, 1994.

[38] S. Nadeem and S. Hussain, "Heat transfer analysis of Williamson fluid over exponentially stretching surface," *Appl. Math. Mech.*, vol. 35, no. 4, pp. 489–502, 2014.

[39] M. Bhatti, A. Shahid, and M. Rashidi, "Numerical simulation of fluid flow over a shrinking porous sheet by successive linearization method," *J. Alex. Eng.*, vol. 55, no. 1, pp. 51–56, 2016.